Structures 78 (2025) 109189

Contents lists available at ScienceDirect

Structures

journal homepage: www.elsevier.com/locate/structures

Mapping and revealing the nature of masonry compressive strength using computational intelligence

Panagiotis G. Asteris [a,*], Georgios A. Drosopoulos [b], Liborio Cavaleri [c], Antonio Formisano [d], Anastasios Drougkas [e], Gabriele Milani [f], Amin Mohebkhah [g], Paulo B. Lourenço [h]

[a] Computational Mechanics Laboratory, School of Pedagogical and Technological Education, Heraklion, Athens GR 14121, Greece
[b] Department of Civil Engineering, International Hellenic University, Serres GR62124, Greece
[c] Department of Engineering, University of Palermo, Italy
[d] Department of Structures for Engineering and Architecture, University of Naples Federico II, P.le V. Tecchio 80, Naples 80125, Italy
[e] Laboratory of Earthquake and Geotechnical Engineering, School of Pedagogical and Technological Education, Heraklion, Athens GR14121, Greece
[f] Department of Architecture, Built Environment and Construction Engineering (ABC), Politecnico di Milano, Piazza Leonardo da Vinci 32, Milan 20133, Italy
[g] Department of Civil Engineering, Faculty of Civil Engineering and Architecture, Malayer University, Malayer, Iran
[h] Department of Civil Engineering, ISISE, University of Minho, Guimarães, Portugal

ARTICLE INFO

Keywords:
Artificial neural networks
Compressive strength
Computational intelligence
Masonry
Optimization algorithms

ABSTRACT

The compressive strength of masonry walls constitutes a significant parameter that strongly influences the structural response of masonry buildings, under either static or dynamic actions. Significant variability is observed in the range of compressive strength values as highlighted by existing experimental investigations. Empirical relations providing the compressive strength also feature significant prediction divergence. This is attributed to large variations in the geometry and type of units, joint thicknesses, materials and building practices. Therefore, the need arises for the accurate prediction of the compressive strength of masonry walls, using data which is accumulated from past experiments. Artificial intelligence tools and machine learning techniques are considered in this study, to leverage the experience from those past experiments in predicting the compressive strength. A dataset of 611 specimens is developed, to the authors' best knowledge comprises the largest dataset assembled for this purpose to date. Different Back Propagation Neural Networks models are trained and tested using the new dataset, leading to an optimal machine learning architecture. Results indicate that the optimal model can provide an improved prediction of the compressive strength as compared to literature proposals. Parameters which drastically affect the compressive strength are highlighted and expressions predicting the compressive strength are discussed.

1. Introduction

Masonry is considered as one of the oldest construction materials, with its usage dated back to 6500 BC [49]. This material has been used in several structural systems, including buildings, arch bridges and monuments. Masonry is also chosen in modern construction, due to its environmental performance, good thermal properties, strength, and durability.

Masonry walls consist of masonry units and mortar, the material connecting the units, applied between their interfaces. Different materials are used for the masonry units, such as clay bricks, concrete blocks and stone blocks formed as solid, hollow or grouted units. Different types of mortar include earth, aerial lime (with or without the addition of pozzolan), hydraulic lime or cement.

There is an inherent complexity in evaluating the compressive response of masonry structures. This is attributed to the heterogeneity and anisotropy induced by the interaction between the masonry units and the mortar interfaces. Several parameters also influence the response of masonry walls, including among others the dimensions and compressive strength of masonry units, the dimensions of the wall, the compressive strength of mortar as well as the type of the units and mortar [25]. Aiming to capture the non-linear response of masonry different approaches have been adopted, including experimental

* Corresponding author.
E-mail addresses: panagiotisasteris@gmail.com, asteris@aspete.gr (P.G. Asteris).

https://doi.org/10.1016/j.istruc.2025.109189
Received 20 January 2025; Received in revised form 2 April 2025; Accepted 11 May 2025
Available online 28 May 2025

Nomenclature

ANN(s)	Artificial Neural Network(s)
ANN-BFGS	Artificial Neural Network optimized by Broyden–Fletcher–Goldfarb–Shanno quasi-Newton algorithm
ANN-ICA	Artificial Neural Network optimized by Imperialist Competitive Algorithm
ANN-LM	Artificial Neural Network optimized by Levenberg-Marquardt algorithm
ANN-PSO	Artificial Neural Network optimized by Particle swarm algorithm
BFGS	Broyden–Fletcher–Goldfarb–Shanno quasi-Newton algorithm
BPNN	Back Propagation Neural Network
Co	Competitive transfer function
compet	MATLAB function for the Competitive (Co) transfer function
f_{bc}	Compressive strength of the masonry unit [in MPa]
f_{mc}	Compressive strength of the mortar [in MPa]
f_{wc}	Compressive strength of wall or prism [in MPa]
hardlim	MATLAB function for the Hard-limit (HL) transfer function
hardlims	MATLAB function for the Symmetric hard-limit (SHL) transfer function
h_w	Height of the wall
ICA	Imperialist Competitive Algorithm
Li	Linear transfer function
LM	Levenberg-Marquardt algorithm
logsig	MATLAB function for the Log-sigmoid (LS) transfer function
LS	Log-Sigmoid transfer function
MAPE	Mean Absolute Percentage Error
MSE	Mean Square Error
NRB	Normalized Radial Basis transfer function
PLi	Positive Linear transfer function
poslin	MATLAB function for the Positive linear (PLi) transfer function
PSO	Particle Swarm Optimization algorithm
purelin	MATLAB function for the Linear (Li) transfer function
R	Pearson correlation coefficient
RA	Regression Analysis
radbas	MATLAB function for the Radial basis (RB) transfer function
radbasn	MATLAB function for the Normalized radial basis (NRB) transfer function
RB	Radial Basis transfer function
satlin	MATLAB function for the Saturating linear (SL) transfer function
satlins	MATLAB function for the Symmetric saturating linear (SSL) transfer function
SM	Soft Max transfer function
softmax	MATLAB function for the Soft max (SM) transfer function
SSE	Sum Square Error
SSL	Symmetric Saturating Linear transfer function
TB	Triangular Basis transfer function
tansig	MATLAB function for the Hyperbolic Tangent Sigmoid (HTS) transfer function
t_b	Masonry unit thickness
t_m	Bed joint thickness
tribas	MATLAB function for the Triangular basis (TB) transfer function
t_w	Thickness of the wall
v_m	Relative volume of mortar
V_m	Volume of mortar
v_u	Relative volume of masonry unit
V_{wall}	Volume of masonry wall

research and numerical modelling [10,77,89]. Often, those approaches lead to semi-empirical equations predicting the compressive response of masonry walls as a function of the compressive strengths of units, mortar and other relevant parameters.

The failure mode of masonry walls under compression is investigated in most experimental studies, highlighting how parameters like the relative strength of the units and the mortar and the interaction of these constituents influence failure. An experimental investigation on concrete masonry prisms presented in [35] indicates that hollow prisms fail when transverse tensile stresses near the mortar - block interface split the block or when compressive stresses lead to crushing of the confined mortar. In [6] it is shown that when the concrete blocks and the mortar of the tested prisms have similar strengths, a rupture failure mode occurs with a vertical crack starting in the middle block of the prism that grows as the loads increase.

In [103] prisms consisting of high strength blocks lead to significant compressive strength increment for increasing compressive strengths of the mortar. For specimens with higher mortar strength, masonry blocks tend to expand laterally more than the mortar, leading to lateral compressive stresses in the blocks, lateral tensile stresses in the mortar, resulting in brittle crushing failure on the blocks. In [108], it is observed that the compressive strength of walls made of Indian brick masonry increases for increasing strength of bricks and mortar, with the effect becoming more obvious for low strength mortar. An experimental study on Pakistani brick masonry walls [73] concludes that failure of the wall is attributed to failure of the brick unit except diagonal tests with poor mortar, where more ductile failure arises along the mortar interfaces.

From the given descriptions, it is apparent that several parameters potentially influence the compressive response of masonry walls, highlighting the complexity of the task. Hence, the need arises to use the accumulated experience from past experiments, in the context of recent advancements in Artificial Intelligence (AI). Within this framework, machine learning (ML) techniques have been introduced to capture the response and predict the failure load and collapse mechanism of masonry structures, using data obtained either experimentally or numerically. Those machine learning tools are used to predict key aspects of the response of masonry structures, such as the failure surfaces of masonry using Artificial Neural Networks (ANNs) [14], the dynamic response of historic masonry buildings considering updating of finite element models using genetic algorithms and machine learning [128], the failure response of masonry walls introducing ANNs in computational homogenization [41], and the failure load and collapse mechanism of masonry arches using ANNs [99]. Recent efforts also involve computer vision and deep learning techniques, that are used to capture the existing failure state of masonry buildings, by introducing image recognition methods [135,140,4,39,80].

In this framework, the investigation of the compressive strength of masonry walls using machine learning techniques is elaborated in recent studies. In [11] ANN models were adopted to predict the compressive strength of masonry walls using 232 experimental datasets, considering as input data the volume fraction and the compressive strength of the masonry unit, the compressive strength of the mortar, the height to thickness ratio of the masonry specimen and the volume ratio of bed joint mortar. In [123] an ensemble artificial intelligence-based method is proposed to predict the compressive strength of hollow concrete block masonry prisms. The models of this study are developed using data derived from 90 relevant experimental investigations published in literature. To predict the non-linear relation between the compressive

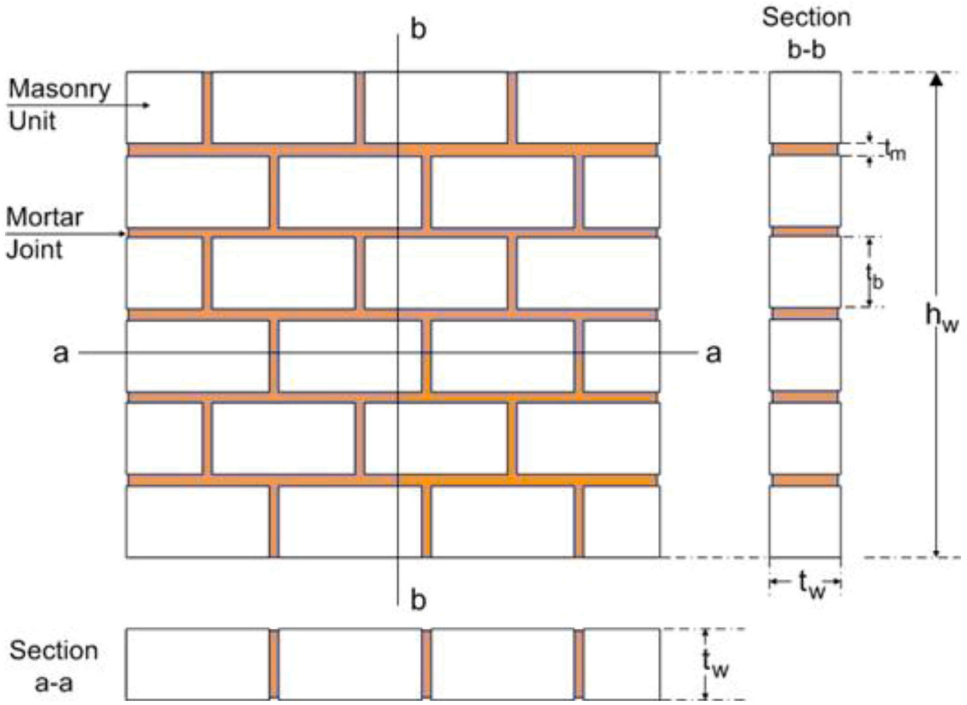

Fig. 1. Geometric notations of masonry walls.

strength of masonry structures and the compressive strengths of bricks and mortar, an ANN model, a fuzzy inference system and a support vector regression model are optimized in [60]. A bat-inspired algorithm is used to extract the best values of weights and biases of the ANN, the membership's functions of the fuzzy inference system, and the user-defined parameters of the support vector regression. In [50] ANNs, combinatorial methods of group data handling (GMDH-Combi), and gene expression programming (GEP) are used to predict the compressive strength of hollow concrete block masonry prisms. These models were trained and tested against 102 data points sourced from the relevant literature. The height to thickness ratio and the compressive strength of the mortar and the blocks were used as input parameters. Further related studies can be found in [92,91,90].

In [12] soft-computing techniques are adopted to evaluate the compressive strength of masonry walls, using a dataset of 401 specimens. Results indicate the most relevant parameters affecting the compressive strength of masonry as well as areas in which more experimental research is needed, particularly masonries with units and/or mortar with a compressive strength higher than 15 MPa. It is also shown that the range of the compressive strengths of masonry prisms is too broad, in particular for higher values of the compressive strength of bricks. Therefore, it is concluded that one significant outcome of the mentioned studies is the variability of the obtained compressive strength in terms of geometric and strength parameters of the constituents, as derived from the used machine learning techniques, semi-empirical equations or experimental research. Hence, a holistic approach is needed, that will aim to predict the compressive strength using the existing experimental data.

The present study attempts to provide a further insight in the compressive strength of masonry, by proposing soft-computing and machine learning techniques. A dataset of 611 specimens derived from past experiments is developed, aiming to enhance the accuracy of previous efforts and consider a range of parameter values not adequately covered in previous studies. A large number of Back Propagation Neural Networks (BPNN) models is trained and tested, leading to an optimal architecture. Input parameters are the masonry unit compressive strength, the mortar compressive strength, the masonry wall height to thickness ratio and the mortar thickness to masonry unit thickness ratio. The output parameter is the compressive strength of masonry, which is subsequently compared with the experimentally derived values for statistical evaluation of model performance.

2. Literature review on masonry compressive strength

In several experimental studies, geometrical parameters and materials properties that influence the compressive strength of masonry prisms are considered. Those include the compressive strength of the masonry unit f_{bc}, the compressive strength of the mortar f_{mc}, the height to thickness ratio h_w/t_w of the specimen, and the mortar thickness to masonry unit thickness ratio t_m/t_b. The pattern of a masonry wall and the relevant geometric parameters are shown in Fig. 1.

One research objective that appears in relevant studies is to investigate how the strengths of the constituent materials, namely the masonry unit and the mortar, influence the compressive strength of masonry. When the compressive strength of mortar is lower than the one of the masonry unit, the behaviour of masonry in compression is governed either by the mortar confined compressive strength or by the strength of the unit under vertical compression and lateral tension, leading to compressive strength values for the masonry in-between the compressive strengths of mortar and the units [12]. On the contrary, when the compressive strength of units is lower than the one of mortar, the compressive response of masonry is controlled by the unit, and is usually lower than the compressive strength of both constituents [113].

It has also been found that mortars with smaller thickness contribute towards increasing the strength of the mortar-brick interface, resulting in the increase of the compressive strength of masonry [12].

2.1. *Available proposals in the literature for strength prediction*

In several research efforts, solutions predicting the compressive strength of masonry walls are presented, considering analytical or semi-empirical mathematical equations. These equations are developed adopting a form of regression, using existing experimental studies. In the simplest case, those equations predict the compressive strength of

Table 1
Empirical equations for the prediction of masonry compressive strength.

Nr	Formula	Reference	Method used
1	$f_{wc} = \frac{1}{3}f_{bc} + \frac{2}{3}f_{mc}$	Engesser [49]	RA
2	$f_{wc} = 0.68{f_{bc}}^{1/2}{f_{mc}}^{1/3}$	Bröcker [29]	RA
3	$f_{wc} = 0.83{f_{bc}}^{0.66}{f_{mc}}^{0.18}$	Mann [84]	RA
4	$f_{wc} = 0.317{f_{bc}}^{0.531}{f_{mc}}^{0.208}$	Hendry, Malek [66]	RA
5	$f_{wc} = 0.275{f_{bc}}^{0.5}{f_{mc}}^{0.5}$	Dayaratnam [40]	RA
6	$f_{wc} = \frac{2}{3}f_{bc} + 0.1f_{mc}$	Tassios [129]	RA
7	$f_{wc} = 0.7f_{bc}^{\frac{1}{2}}f_{mc}^{\frac{1}{3}}$	Tassios [129]	RA
8	$f_{wc} = 0.3f_{bc}$	Bennett et al. [24]	RA
9	$f_{wc} = 0.4{f_{bc}}^{0.7}{f_{mc}}^{0.435}$	Cuomo, Badalà [38]	RA
10	$f_{wc} = 0.3266f_{bc} \times (1 - 0.0027f_{bc} + 0.0147f_{mc})$	Dymiotis, Gutlederer [44]	RA
11	$f_{wc} = 0.63{f_{bc}}^{0.49}{f_{mc}}^{0.32}$	Kaushik et al. [69]	RA
12	$f_{wc} = 0.317{f_{bc}}^{0.866}{f_{mc}}^{0.134}$	Gumaste et al. [64]	RA
13	$f_{wc} = 0.225{f_{bc}}^{0.855}{f_{mc}}^{0.146}$	Gumaste et al. [64]	RA
14	$f_{wc} = 0.6{f_{bc}}^{0.65}{f_{mc}}^{0.25}$	CTE [37]	RA
15	$f_{wc} = 0.35{f_{bc}}^{0.65}{f_{mc}}^{0.25}$	Christy et al. [36]	RA
16	$f_{wc} = 0.53f_{bc} + 0.93f_{mc} - 10.32$	Garzón-Roca et al. [57]	RA
17	$f_{wc} = \frac{84}{1 + e^{3.6 - 0.077f_{mc} - 0.034f_{bc}}} - 0.36$	Garzón-Roca et al. [57]	ANNs
18	$f_{wc} = 0.75{f_{bc}}^{0.75}{f_{mc}}^{0.31}$	Lumantarna et al. [81]	RA
19	$f_{wc} = 0.886{f_{bc}}^{0.75}{f_{mc}}^{0.18}$	Sarhat, Sherwood [118]	RA
20	$f_{wc} = 13.04 + 0.402f_{bc}$	Fortes et al. [53]	RA
21	$f_{wc} = 1.34{f_{bc}}^{0.1}{f_{mc}}^{0.33}$	Basha, Kaushik [23]	RA
22	$f_{wc} = 0.69{f_{bc}}^{0.6}{f_{mc}}^{0.35}$	Kumavat [75]	RA
23	$f_{wc} = 0.25{f_{bc}}^{1.09}{f_{mc}}^{0.12}$	Thamboo, Dhanasekar [134]	RA
24	$f_{wc} = 0.09f_{mc} + 3.92$	Yang et al. [141]	RA
25	$f_{wc} = 0.52{f_{bc}}^{0.534}{f_{mc}}^{0.466}$	Boffill et al. [26]	RA
26	$f_{wc} = 0.6{f_{bc}}^{0.7}{f_{mc}}^{0.4}$	Moayedian, Hejazi [94]	RA
27	$f_{wc} = 0.6{f_{bc}}^{0.6}{f_{mc}}^{0.3}$	Moayedian, Hejazi [94]	RA
28	$f_{wc} = 0.6{f_{bc}}^{0.5}{f_{mc}}^{0.2}$	Moayedian, Hejazi [94]	RA
29	$f_{wc} = 0.6{f_{bc}}^{0.4}{f_{mc}}^{0.2}$	Moayedian, Hejazi [94]	RA

f_{wc} is the masonry compressive strength; f_{bc} is the masonry unit compressive strength; f_{mc} is the mortar compressive strength; RA: Regression Analysis; ANNs: Artificial Neural Networks

masonry walls, using as input the compressive strengths of the masonry unit and the mortar. A list of those equations and relevant literature sources are provided in Table 1.

As seen in Table 1, parameters like the width to thickness and height to thickness ratios of masonry, the volume fraction of the masonry unit, the thickness of mortar joint to thickness of the masonry unit ratio, the effect of biaxial or triaxial stress, the effect of interfacial transition zone and bond strength, and others, are not considered. To address this issue, some of these parameters have been considered in relevant regression studies, resulting in additional empirical equations predicting the compressive strength of masonry walls as shown in Table 2. In those equations, parameters like the ratio of bedded web area to total web area of hollow block units, the width to thickness and the height to thickness (slenderness) ratios, the volume fraction of masonry unit (masonry unit volume to masonry wall volume ratio) and the volume ratio of bed joint to mortar (volume fraction of mortar in horizontal joints to volume fraction of mortar in horizontal and vertical joints ratio) as well as compressive strength of grout have been included.

While semi-empirical equations predicting the compressive strength of masonry walls considering some of the mentioned parameters have been proposed in older studies, such as for instance in [129,130], relevant efforts have been conducted in recent investigations. In [103] multiple nonlinear regression analysis is implemented, providing analytical equations for the compressive strength of masonry walls consisting of concrete blocks, cement-lime mortar and grout. For the prediction of the compressive strength of masonry, several equations are proposed as a function of the compressive strengths of the masonry unit (f_{bc}), the mortar (f_{mc}) and the grout (f_{gc}), for three variations of the first

Table 2
Empirical equations for the prediction of masonry compressive strength using additional input parameters.

Nr	Formula	Reference	Method used
1	$f_{wc} = f_{bc}(4 + 0.1f_{mc})/(12 + \frac{5h_w}{t_w}) + 2$	Tassios [129]	RA
2	$f_{wc} = 0.30f_{bc} + 0.20f_{mc} + 0.25f_{gc}$	Khalaf et al., [72]	RA
3	$f_{wc} = -1.56 + 0.296f_{mc} + 0.524f_{bc} + 4.149r$	Ramamurthy et al., [111]	RA
4	$f_{wc} = A(400 + Bf_{bc})$	[2]	RA
5	$f_{wc} = 1.57\ln(f_{mc}) + 0.75f_{bc} + 5.81\ln(\frac{f_{gc}}{f_{bc}})$	Köksal et al., [74]	RA
6	$f_{wc} = \frac{0.54f_{bc}^{1.06}f_{mc}^{0.004}VF_{bc}^{3.3}VR_{mcH}^{0.6}}{h_w/t_w^{0.28}}$	Thaickavil, Thomas [131]	RA
7	$f_{wc} = f_{bc}\frac{4 + 0.1f_{mc}}{1.5l_w/t_w + 5h_w/t_w}$	Khan et al., [73]	RA

f_{wc} is the masonry compressive strength; f_{bc} is the masonry unit compressive strength; f_{mc} is the mortar compressive strength; r is ratio of bedded web area to total web area of hollow block units; l_w/t_w and h_w/t_w are the width to thickness and the height to thickness (slenderness) ratios; VF_{bc} and VR_{mcH} are the volume fraction of masonry unit (masonry unit volume to masonry wall/prism volume ratio) and the volume ratio of bed joint to mortar (volume fraction of mortar in horizontal joints to volume fraction of mortar in horizontal and vertical joints ratio); A is equal to 1 for inspected masonry and B is equal to 0.2 for Type N mortar per ASTM C270–24 [17]; f_{gc} is the compressive strength of grout; RA: Regression Analysis

Table 3
Empirical equations predicting the compressive strength of masonry adopted by international codes and standards.

Nr	Formula	Reference
1	$f_{wc} = k_h k_m {f_{bc}}^{0.5}$	AS Committee 3700–2018 [9]
2	$f_{wc} = 2.758 + 0.2 f_{bc}$	[2,100]
3	$f_{wc} = \begin{cases} K {f_{bc}}^{0.7} {f_{mc}}^{0.3}, & 3mm \le t_m \le 15mm \\ K {f_{bc}}^{0.85}, & t_m \le 3mm \end{cases}$	EN 1996–1–1 [47]

f_{wc} is the masonry compressive strength; f_{bc} is the masonry unit compressive strength; f_{mc} is the mortar compressive strength; k_h is a factor in Australian code AS 3700–2018 that accounts for the ratio of unit thickness to mortar joint thickness, which should not exceed the value of 1.3; k_m is also a factor in Australian code AS 3700–2018 that accounts for the type of unit, the mortar compressive strength and the bedding type; K is a constant in Eurocode 6, 2005 (EN 1996–1–1) formula, which may be modified according to the National Annex for different countries. The value of this constant in the UK is 0.52 while in Greece K values range between 0.35 and 0.55 depending on the material and on the group of the masonry unit, the type of the mortar (e.g. general purpose mortar, thin layer mortar or mortar made with lightweight aggregates).

two, namely Eq. (1) for mortar weaker than the masonry unit, Eq.(2) for intermediate mortar strength and Eq. (3) for high strength mortar.

$$f_{wc} = 0.011 f_{bc} + 1.188 f_{mc} + 0.548 f_{gc}, \qquad f_{mc} \le 0.4 f_{bc} \tag{1}$$

$$f_{wc} = 0.444 f_{bc} + 0.190 f_{mc} + 0.539 f_{gc}, \qquad 0.4 f_{bc} < f_{mc} \le f_{bc} \tag{2}$$

$$f_{wc} = 0.310 f_{bc} + 0.390 f_{mc} + 0.415 f_{gc}, \qquad f_{mc} > f_{bc} \tag{3}$$

In [50] artificial intelligence algorithms have been used to provide a prediction of the compressive strength of hollow concrete block masonry prisms according to Eq. (4). To train and test the mentioned models, 102 samples found in literature were used, considering as input the height to thickness ratio (h_w/t_w) as well as the compressive strength of mortar (f_{mc}) and concrete blocks (f_{bc}), according to:

$$f_{wc} = -47.44 + 1.93 f_{bc} + 5.23 f_{mc} - \frac{4.84 h_w}{t_w} - 0.09 f_{bc} f_{mc} - \frac{5.32 f_{bc}}{f_{mc}} - \frac{52.47 f_{mc}}{f_{bc}} + \frac{2439.49}{f_{bc} f_{mc}} + \frac{130.13 \left(\frac{h_w}{t_w}\right)}{f_{bc}} + \frac{1007.7}{f_{bc} \left(\frac{h_w}{t_w}\right)} - \frac{1.63 f_{mc}}{\left(\frac{h_w}{t_w}\right)} + \frac{217.39}{f_{mc}} \tag{4}$$

The conducted research on the field has also been adopted by international building codes providing the compressive strength of masonry walls, using characteristic values (or the 5 % quartile). In Table 3 analytical equations of the compressive strength of masonry proposed by international codes and standards are presented.

In [12] it is shown that a great variability for the predictions of the compressive strength of masonry using the mentioned semi-empirical equations is obtained, for a range of masonry unit compressive strength values.

2.2. Short review of soft computing models for strength prediction

In Table 4 published studies are provided, predicting the compressive strength of masonry walls using machine learning approaches. As seen in Table 4, those approaches include artificial neural networks (ANNs), ensemble intelligent predictive models, fuzzy inference systems (FIS), support vector regression models (SVR), combinatorial methods of group data handling (GMDH-Combi), gene expression programming models (GEP), adaptive neuro-fuzzy inference systems (ANFIS), fuzzy logic models (FL), genetic programming models (GP), decision tree models (DT), ridge regression models (RR), random forest regression models (RFR), and others. In [61], a deep learning Convolutional Neural Network, usually adopted for image recognition tasks, is used to predict the compressive strength of masonry walls. An approach of integrating various machine learning techniques aiming to provide optimized predictions of the compressive strength, known as Committee Machine

Table 4
Literature survey table for studies on masonry compressive strength prediction using AI (GUI is Graphical User Interface).

References	Models used	Input parameters	Samples	Accuracy (Coefficient of determination, R^2)	Provided formula or/and GUI
Garzón-Roca et al. [57]	ANN & FL	f_{bc}, f_{mc}	96	Training: 0.9910, Testing: 0.9890	Weights and biases of ANN model & Formula
Zhou et al. [144]	ANN & ANFIS	f_{bc}, f_{mc}, h_w/t_w	102	Training: 0.9714, Testing: 0.9693	-
Mishra et al. [90]	SVMs	f_{bc}, RH, UPV	44	0.9600	Formula
Mishra et al. [91]	ANN & SVR & ANFIS	RH, UPV	44	0.9702	Formula
Mishra et al. [92]	SR & ANN & ANFIS	RH, UPV	44	0.9710	Formula
Sharafati et al. [123]	BGR	f_{bc}, f_{mc}, h_w/t_w	90	0.9700	-
Asteris et al. [12]	ANN & GP	f_{bc}, f_{mc}, t_m, t_b, h_w/t_w, t_m/t_b	401	0.8987	Weights and biases of ANN model & Formula
Gholami, Gholami [60]	Integrating ANN & FIS & SVR using CM	f_{bc}, f_{mc}	96	Training: 0.9855, Testing: 0.9739	-
Fakharian et al. [50]	ANN & GMDH-Combi & GEP	f_{bc}, f_{mc}, h_w/t_w	102	0.9030	Weights and biases of ANN model & Formula
Sathiparan, Jeyananthan [119]	LR & DT & RR & RFR & ANN & XG Boost	t_l/t_w, t_b/t_w, t_m/t_b, h_w/t_w, f_{bc}, f_{mc}	540	0.9500	-
Gholami et al. [61]	Integrating OCNN & ELM & DT using a PLCM	f_{bc}, f_{mc}	96	0.9922	-

f_{bc}: Masonry unit compressive strength; f_{mc}: Mortar compressive strength; h_w/t_w: Height to thickness (slenderness) ratio of the wall; t_m/t_b: Mortar thickness to masonry unit thickness ratio; t_l/t_w: Masonry unit length to thickness ratio; t_b/t_w: Masonry unit height to thickness ratio; VF_{bc} and VR_{mcH}: Volume fraction of masonry unit (masonry unit volume to masonry wall volume ratio) and volume ratio of bed joint to mortar (volume fraction of mortar in horizontal joints to volume fraction of mortar in horizontal and vertical joints ratio); RH: Rebound hammer number; UPV: Ultrasonic pulse velocity ANN: Artificial Neural Network; BGR: Ensemble intelligent predictive model called Bagging Regression; FIS: Fuzzy Inference System; SVR: Support Vector Regression; GMDH-Combi: Combinatorial methods of group data handling; GEP: Gene Expression Programming; SVMs: Support Vector Machines; ANFIS: Adaptive neuro-fuzzy inference system; SR: Statistical Regression; FL: Fuzzy Logic; GP: Genetic Programming; LR: Linear Regression; DT: Decision Tree; RR: Ridge Regression; RFR: Random Forest Regression; OCNN: Optimized Convolutional Neural Network; ELM: Extreme Learning Machine; CM: Committee Machine; PLCM: Power-Law Committee Machine

Table 5
Data from experiments published in literature.

Nr.	Reference	Number of Samples	Masonry Compressive Strength in MPa	Type of Masonry Units
1	[131]	48	0.73–2.80	Cement stabilized earth brick and burnt clay brick
2	[113]	1	5.80	Soft clay wire-cut brick
3	[125]	8	2.07–10.26	Burnt clay brick and concrete brick
4	[144]	12	5.48–14.60	Hollow concrete block
5	[21]	1	2.82	Poor quality brick used in south India with quite low compressive strength
6	[138]	1	4.42	Solid concrete block
7	[81]	12	6.19–30.79	Vintage solid clay brick
8	[102]	3	1.92–2.43	Handmade burnt clay brick
9	[132]	4	6.90–10.10	Hollow concrete block
10	[137]	12	0.65–3.20	Stabilized mud block
11	[114]	3	3.34–3.85	Compressed earth block
12	[69]	8	2.90–7.20	Local clay brick in India (designated as m, b, s, and o)
13	[64]	6	1.25–10.00	Table moulded brick and wire-cut brick
14	[96]	6	7.54–11.70	Hollow concrete block
15	[28]	2	9.90–13.50	Solid clay brick
16	[20]	4	10.89–16.89	Solid clay brick
17	[68]	1	3.50	Ohio stone
18	[67]	1	18.20	Burnt clay half size brick
19	[136]	29	3.90–26.90	Red soft mud, yellow wire-cut, Poriso perforated soft mud brick, calcium silicate brick and red soft mud bricks
20	[87]	2	19.70–27.00	Modular cored unit
21	[54]	23	8.40–37.49	Solid bricks and extruded bricks
22	[64]	6	1.18–12.60	Table moulded brick and wire-cut brick
23	[104]	26	6.98–16.46	Hollow concrete blocks
24	[42]	6	9.05–13.80	Solid clay bricks
25	[59]	16	1.80–11.15	Hollow concrete blocks
26	[139]	3	5.01–6.32	Compressed cement blocks
27	[22]	3	10.00–12.00	Hollow concrete blocks
28	[134]	20	1.22–7.27	Clay bricks and compressed earth blocks
29	[98]	1	7.66	Solid clay brick
30	[109]	6	5.96–7.90	Solid clay bricks
31	[101]	1	9.84	Solid clay bricks
32	[62]	1	22.90	Granite stone units
33	[143]	11	11.57–15.86	Hollow calcium silicate blocks
34	[30]	2	1.84–2.80	Compressed earth blocks
35	[107]	4	2.62–4.05	Compressed earth blocks
36	[78]	1	5.37	Perforated concrete blocks
37	[88]	1	2.80	Perforated concrete blocks
38	[79]	1	5.26	Perforated clay bricks
39	[65]	2	5.44–5.95	Perforated concrete blocks
40	[86]	2	5.98–7.54	Solid clay bricks
41	[95]	8	7.54–11.70	Hollow concrete blocks
42	[112]	1	2.40	Vertical hollow concrete bricks
43	[32]	3	7.42–9.05	Hollow clay brick
44	[33]	3	2.53–4.20	Hollow calcarenite bricks
45	[34]	1	1.74	Hollow lightweight concrete
46	[27]	3	6.93–15.38	Clay bricks
47	[63]	4	1.57–11.03	Clay bricks, dense aggregate concrete and autoclaved aerated concrete
48	[90]	38	1.09–6.07	Solid clay bricks type i, ii and iii (unplastered)
49	[56]	7	0.45–0.97	Horizontal hollow clay bricks
50	[55]	9	0.54–1.28	Horizontal hollow clay bricks
51	[124]	1	4.21	Hollow concrete blocks
52	[117]	1	4.49	Hollow concrete blocks
53	[83]	9	4.35–12.04	Solid wall ceramic unit, hollow walled ceramic unit and concrete unit
54	[97]	4	5.25–9.27	Concrete unit
55	[96]	1	8.24	Concrete unit
56	[110]	4	2.16–3.10	Clay bricks and concrete blocks
57	[105]	2	10.58–11.54	Solid burnt clay bricks
58	[35]	1	19.24	Hollow concrete blocks
59	[43]	12	12.76–25.41	Hollow concrete blocks
60	[71]	11	13.22–26.00	Hollow concrete blocks
61	[104]	28	13.70–31	Hollow concrete blocks
62	[106]	2	10.08–11.74	Hollow concrete blocks
63	[111]	11	6.63–13.76	Hollow concrete blocks
64	[115]	12	11.31–22.69	Hollow concrete blocks
65	[116]	9	14.25–27	Hollow concrete blocks
66	[122]	2	22.20–25.70	Hollow concrete blocks
67	[73]	12	3.71–6.84	First-class fire-burnt clay bricks
68	[127]	9	2.26–3.72	Autoclaved aerated concrete (AAC) blocks
69	[142]	12	5.80–1390	Solid concrete blocks and hollow concrete blocks
70	[108]	6	5.96–9.39	Hand-moulded solid clay bricks
71	[1]	6	23.38–31.16	Concrete blocks
72	[52]	11	19.50–33.30	High-strength concrete masonry units
73	[121]	8	5.88–7.31	Solid clay bricks
74	[6]	3	6.71–7.33	Concrete blocks
75	[120]	9	2.13–2.98	Solid fired-clay bricks
76	[85]	12	5.60–23.80	Hollow concrete blocks
77	[133]	4	2.80–9.80	Thin layer mortared clay masonry bricks
78	[103]	12	5.60–18.30	Hollow concrete blocks
79	[141]	16	4.94–6.00	Concrete bricks
80	[58]	1	0.98	Solid brick walls
81	[93]	3	1.61–1.77	Masonry bricks
	Total	**611**	**0.45–33.30**	

(CM), is proposed in [60,61].

The input parameters for the chosen machine learning techniques, the number of dataset samples and the coefficient of determination (R^2) corresponding to each of the presented studies, are also included in Table 4. As seen, most of the studies consider as input the compressive strength of the masonry unit and the mortar, f_{bc} and f_{mc}, respectively. In some studies, the height to thickness (slenderness) ratio of masonry, h_w/t_w, and the mortar thickness to masonry unit thickness ratio, t_m/t_b, are among the input parameters. In [92,91,90] non-destructive test parameters like the rebound hammer number (RH) and the ultrasonic pulse velocity (UPV) are considered as inputs.

For the majority of the studies in Table 4, fewer than 100 dataset samples are used to train and test the adopted machine learning methods, while the largest dataset sample is 540. In some of those studies, a formula is proposed to predict the compressive strength of masonry walls, as an output of the regression analysis.

Table 6
Statistics of the parameters involved in modelling masonry compressive strength.

Nr.	Variable	Symbol	Unit	Category	Statistics				
					Min	Average	Max	STD	CV
1	Masonry unit compressive strength	f_{bc}	MPa	Input	2.30	18.77	74.90	15.61	0.83
2	Mortar compressive strength	f_{mc}	MPa	Input	0.30	10.23	32.00	6.06	0.59
3	Masonry height to thickness ratio	h_w/t_w	-	Input	1.15	3.31	8.60	1.22	0.37
4	Mortar thickness to masonry unit thickness ratio	t_m/t_b	-	Input	0.01	0.11	0.33	0.07	0.61
5	Masonry compressive strength	f_{wc}	MPa	Output	0.45	9.42	33.30	7.46	0.79

3. Materials and methods

This section presents the methodology followed for the development and formulation of a computational mathematical model for estimating the compressive strength of masonry, as well as the database used for the training, development, and validation of the model. Special emphasis is given to the compilation of the experimental database and the parameters used to simulate the behaviour of masonry, particularly those parameters that influence its compressive strength. Additionally, the different techniques used for the formation of the different models are listed in detail. Finally, the statistical methodology used for establishing the optimal model is presented.

3.1. Compilation of the database

It is common practice for most researchers involved in the formulation and development of predictive computational models to focus more on the computational methods and techniques used, and less on the database used for the development, training, and testing of the model's performance and reliability. The authors of this paper firmly believe the opposite. The authors maintain that the primary factor determining the reliability of a predictive computational model lies in the accuracy and comprehensiveness of the database used to describe the phenomenon under study, without neglecting the importance of the computational method. No matter how innovative or advanced a computational technique is, it cannot lead to a reliable predictive model unless it is supported by a reliable and representative database. This underlines and reaffirms the well-known adage from computer science: "garbage in, garbage out."

Given the importance of the database, it is considered useful and appropriate to briefly present the key principles that should be followed when compiling a reliable and comprehensive database. A reliable database consists of true and trustworthy data while also ensuring that the data adequately and statistically cover all possible values that each variable in the studied problem can take. Furthermore, when collecting experimental data, it is crucial to select data from experiments conducted in certified and credible laboratories, adhering to all relevant international standards, such as [16,18,15,48,45] and [46], including the preparation and storage of specimens under appropriate environmental conditions.

Based on the above considerations, a comprehensive experimental database was compiled to develop and formulate an optimal and reliable computational model for estimating the compressive strength of masonry. This database consists of 611 data points collected from 81 published experimental studies, which are listed in Table 5. To the best of the authors' knowledge, this experimental database is the largest ever compiled and used for studying the compressive strength of masonry. The database is defined by the four input (f_{bc}, f_{mc}, h_w/t_w and t_m/t_b.) and single output parameters (f_{wc}). In Table 5, besides the authors of each study used for the compilation of the experimental database, the number of samples and the range of compressive strength values studied are also provided.

Table 6 presents the aggregated statistical data for the entire database compiled from the 81 experimental studies listed in Table 5. Specifically, the table shows the minimum (Min), average, and maximum (Max) values, as well as the Standard Deviation (STD) and Coefficient of Variation (CV) for each parameter involved in the problem, which determines the compressive strength of masonry. In addition to the statistical parameters, Fig. 2 displays the histograms of the parameters used for predicting the compressive strength of masonry, as well as the relation between each parameter and the compressive strength of masonry, for all cases in the database. The histograms are accompanied by a fitted normal distribution for a clearer visualisation of the distribution of the incidence frequency of these parameters. Both Table 6 and Fig. 2 are capital as they define the validity range of soft computing models trained and developed for estimating masonry compressive strength. This is a crucial issue and will be further discussed in a subsequent section titled "*Limitations and Future Research*."

3.2. Methodology

This section provides a detailed and in-depth description of the methodology followed to identify the optimal soft computing model for estimating the compressive strength of masonry. The key steps of the methodology are as follows:

I. Data Splitting and Normalization: The experimental database, consisting of 611 datasets, was divided into two subsets: 489 datasets (80 %) were used for model training, and the remaining 122 datasets (20 %) were used for model testing. It is important to note how the data was split. The most significant disadvantage of splitting data into a single training set and a single test set is the possibility that the test set may not follow the same class distribution as the overall data, and some numerical features may not have the same distribution in the training and test sets. Considering this, the datasets were initially sorted in descending order based on the masonry compressive strength value, which is the output parameter of the soft computing models. According to the authors' experience, this technique leads to more reliable results. Subsequently, the 80/20 split of the sorted database was performed using the k-fold cross-validation technique with 5 folds [5]. This data splitting process was carried out with normalization of the data using six different classical normalization methods.

II. Simulation Method: To estimate the compressive strength of masonry, Back Propagation Neural Networks (BPNN) models were utilized and trained using (i) four different purely mathematical and nature-inspired optimization algorithms widely used in the literature: Levenberg-Marquardt (LM) algorithm [76], Broyden–Fletcher–Goldfarb–Shanno (BFGS) algorithm [51], Particle Swarm Optimization (PSO) algorithm [70], and the Imperialist Competitive Algorithm (ICA) [19], (ii) architectures with 1 hidden layer, (iii) architectures with 1–30 neurons per hidden layer, with a step of 1, as opposed to using semi-empirical formulas that have been proposed for determining the number of neurons and are commonly used by most researchers [126], and (iv) 12 different transfer functions, leading to 144 (12^2) different combinations for architectures with 1 hidden layer. It is worth noting that most researchers use at most four transfer functions, which makes the evaluation of optimization algorithms

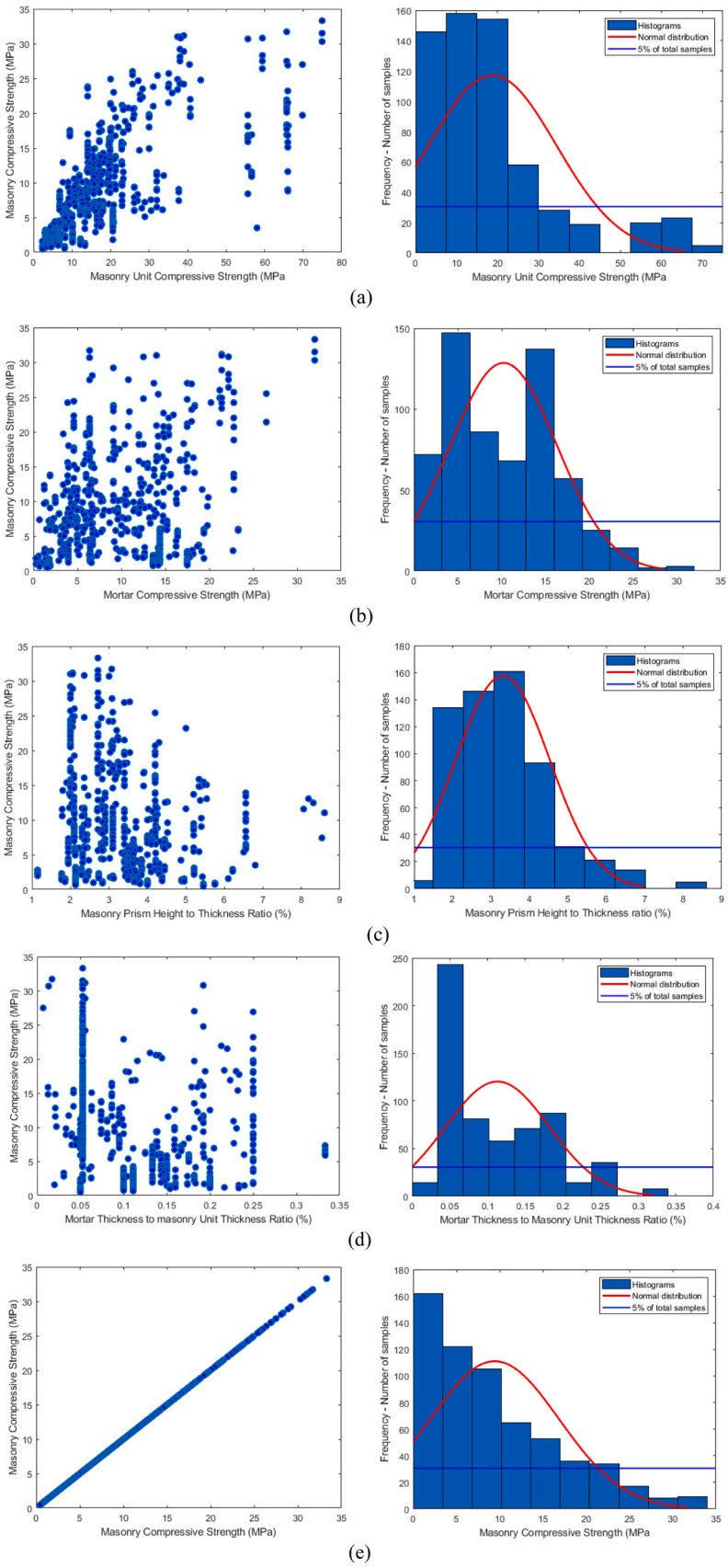

Fig. 2. Histograms of parameters used for the prediction of masonry compressive strength for: (a) Masonry compressive strength (f_{wc}) vs Unit compressive strength, (b) Masonry compressive strength (f_{wc}) vs Mortar compressive strength, (c) Masonry compressive strength (f_{wc}) vs Masonry height to thickness (h_w/t_w) ratio, (d) Masonry compressive strength (f_{wc}) vs Mortar thickness to masonry unit thickness (t_m/t_b) ratio, and (e) Masonry compressive strength (f_{wc}).

Table 7
Best ANN architectures for each one optimization algorithm based on RMSE performance index for Testing Datasets.

Ranking	Model	Architecture	Performance Indices						Comments
			Testing Datasets		Training Datasets		All Datasets		
			R^2	RMSE (MPa)	R^2	RMSE (MPa)	R^2	RMSE (MPa)	
1	ANN-LM	4–9–1	0.9615	2.1083	0.9546	2.2235	0.9557	2.2009	Normalization Technique: Minmax [0.00, 1.00] Cost Function: MSE Transfer function at the hidden layer: radbas Transfer function at the output layer: logsig
2	ANN-BFGS	4–14–1	0.9560	2.2071	0.9623	2.0289	0.9609	2.0657	Normalization Technique: Minmax [−1.00, 1.00] Cost Function: SSE Transfer function at the hidden layer: tansig Transfer function at the output layer: purelin
3	ANN-PSO	4–9–1	0.9201	3.4068	0.8888	3.8681	0.8947	3.7811	Normalization Technique: Minmax [0.00, 1.00] Cost Function: MSE Transfer function at the hidden layer: tansig Transfer function at the output layer: satlins Population: 30
4	ANN-ICA	4–18–1	0.9182	3.4123	0.8917	3.8334	0.8967	3.7536	Normalization Technique: Minmax [0.00, 1.00] Cost Function: MSE Transfer function at the hidden layer: tansig Transfer function at the output layer: satlins Population: 50 Empires: 6

ANN-LM: Artificial Neural Network optimized by Levenberg-Marquardt algorithm
ANN-BFGS: Artificial Neural Network optimized by Broyden–Fletcher–Goldfarb–Shanno quasi-Newton algorithm
ANN-PSO: Artificial Neural Network optimized by Particle swarm optimization algorithm
ANN-ICA: Artificial Neural Network optimized by Imperialist Competitive Algorithm

incomplete and often leads to incorrect conclusions. This will be discussed and demonstrated in the next section, where the results of this study will be presented. For brevity, the full set of parameters used is thoroughly discussed in the document titled *Parameters of ANNs*, which has been appended as supplementary material to this manuscript.

III. Optimal Forecasting Model: The combination of the above parameters resulted in the training and development of many different architectures. All these architectures were evaluated and ranked based on their performance, which was determined using classic and widely accepted performance indices, such as the root mean square error (RMSE), the mean absolute percentage error (MAPE), and the coefficient of determination (R^2) [3]. Briefly, the root mean square error (RMSE) is used to provide the square root of the second power of the difference between predicted and experimental values. The mean absolute percentage error (MAPE) represents the absolute error of the prediction. The coefficient of determination (R^2) measures how close to the linear correlation the prediction and the target values are. VAF calculates the Variance Accounted For between predicted and target values. Additionally, the a20-index, recently proposed [13,7,8], and widely adopted, was applied for the assessment of the developed models. The a20-index is defined according to Eq. (5):

$$a20 - \text{index} = \frac{m20}{M} \tag{5}$$

where M is the number of dataset samples and m20 is the number of samples with a value of (experimental value)/(predicted value) ratio between 0.80 and 1.20. The adoption of the a20-index within the ± 20 % range is justified by the high coefficient of variation observed in the results of compression tests of masonry specimens. The a20-index ranges from 0 to 1, with higher values indicating better performance, and for an ideal predictive model, the a20-index is expected to be close to 1.

IV. Assessment of the Contribution of Each Feature to the Prediction: One of the primary goals of this study is to evaluate the parameters involved in the problem based on their influence on the compressive strength of masonry. For this purpose, using the optimal developed model from the previous step and the SHapley Additive exPlanations (SHAP) method proposed by Lundberg and Lee in 2017 [31,82], the importance of each input parameter on the output parameter is determined and ranked according to their influence from the most to the least significant.

V. Mapping and Revealing the Nature of Masonry Compressive Strength: In this final step of the methodology, using the optimal developed model, a set of graphs is constructed. These graphs reveal the highly nonlinear nature of masonry and demonstrate their usefulness for practicing engineers in the design process of masonry structures.

4. Results and discussion

4.1. Training and development of ANN models

Following the methodology detailed in the previous section, BPNN (Back Propagation Neural Network) models were designed and trained for the estimation of masonry compressive strength. Specifically, using the parameters outlined in the supplementary materials titled *Parameters of ANNs*, a total of 1555,200 different neural network architectures were trained and developed.

The top 20 architectures, based on the RMSE (Root Mean Square Error) performance index for Testing Datasets, were identified for each of the four optimization algorithms. Additionally, the top 20 architectures across all four optimization algorithms are provided in the Spreadsheet file titled *Top 20 ANN Architectures*, which is appended as supplementary material to this work. Furthermore, Table 7 presents the optimal architecture for each of the four optimization algorithms.

Based on the results presented in the Top 20 architectures for each one of the four optimization algorithms, the following key findings are revealed during the modelling of masonry compressive strength:

- Optimization Algorithms: The best performing optimization algorithm was the Levenberg-Marquardt algorithm, followed by the Broyden–Fletcher–Goldfarb–Shanno (BFGS) quasi-Newton algorithm, the Particle Swarm Optimization (PSO) algorithm, and the Imperialist Competitive Algorithm (ICA),

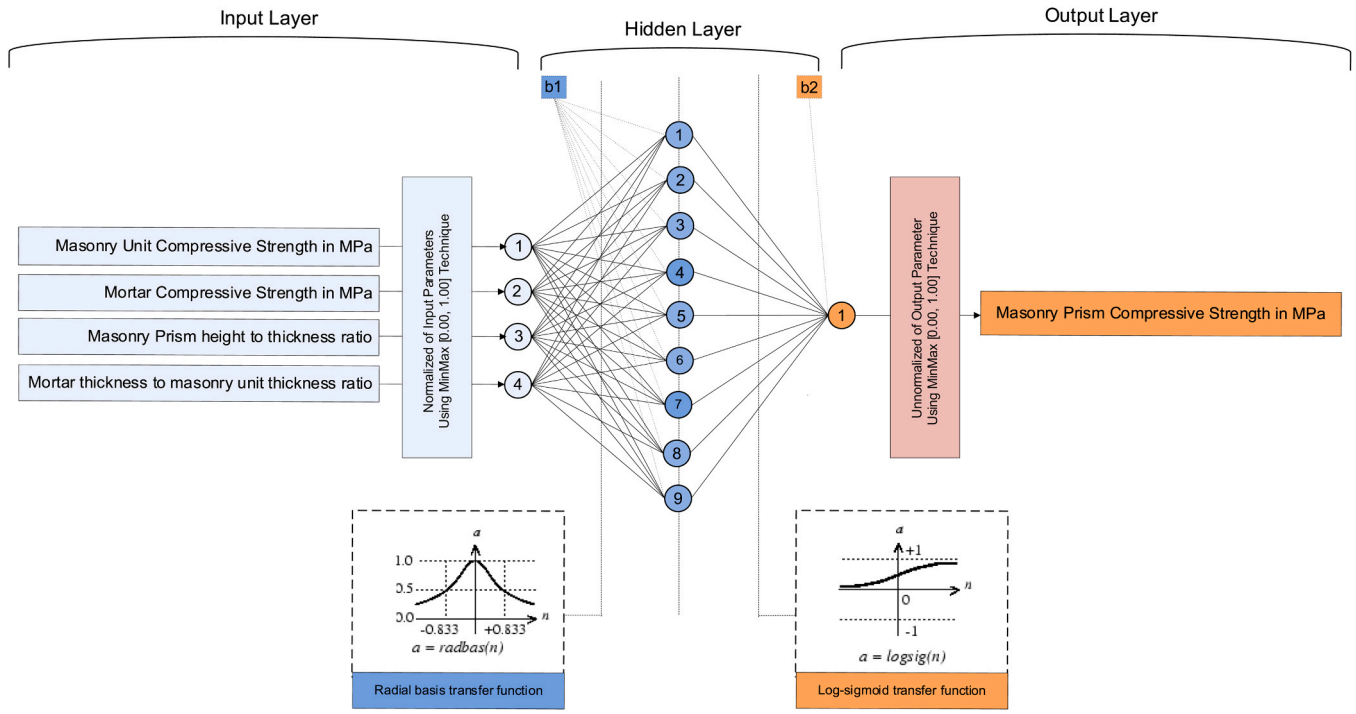

Fig. 3. Architecture of the optimal ANN-LM 4–9–1 model.

Table 8
Summary of prediction capability of the optimum ANN-LM 4–9-1 model.

Model	Datasets	Performance Indices				
		a20-index	R^2	RMSE (MPa)	MAPE	VAF
ANN-LM4–9–1	Training	0.5072	0.9546	2.2235	0.3159	91.1135
	Testing	0.5082	0.9615	2.1083	0.3391	92.0625
	All	0.5074	0.9557	2.2009	0.3205	91.2896

- Transfer Functions: The superior transfer function for the hidden layer was found to be the Radial Basis (RB) function, followed by the Softmax (SM) transfer function. It is worth noting that these two transfer functions are rarely used by researchers. For the output layer, the dominant transfer functions were, in order, the Log-sigmoid (LS) transfer function, the Radial Basis (RB) transfer function, the Symmetric Saturating Linear (SL) transfer function, and the Linear (Li) transfer function.
- Normalization Techniques: The Minmax normalization technique in the range [0.00, 1.00] was found to be the most effective for data normalization,
- Neurons Per Layer: The optimal number of neurons per layer varied significantly depending on the optimization algorithm used. This finding suggests that the semi-empirical formulas commonly proposed in the literature for determining the number of neurons are not reliable.

These results underscore the complexity and specificity required in optimizing ANN models for predicting masonry compressive strength, highlighting the importance of careful selection of network architecture, transfer functions, and normalization techniques.

4.2. Optimal ANN model

Among the trained and developed models presented in the previous subsection, the optimal ANN model, based on the RMSE value of the Testing Datasets, is the ANN-LM 4–9–1 model. This model was optimized using the Levenberg-Marquardt algorithm. Specifically, the optimal ANN-LM 4–9–1 model (Fig. 3) consists of a structure with four input parameters, 9 neurons in the hidden layer, and employs the Minmax normalization technique in the range [0.00–1.00]. The Radial Basis (RB) transfer function is used in the hidden layer, while the Log-sigmoid transfer function is utilized in the output layer.

Table 8 presents the values of five performance indices achieved by the developed and proposed optimal ANN-LM 4–9–1 model. It is noteworthy that all performance indices show better values for the Testing Datasets compared to those for the Training Datasets. This observation is particularly important as it indicates that the model does not suffer from the common overfitting problem. This finding will be further discussed in a subsequent section, along with additional evidence supporting that no overfitting occurred during the model training.

The diagram in Fig. 4, along with the performance indices, is used to assess the reliability and performance of the optimal ANN model. It is confirmed that the developed optimal model is a reliable tool for predicting masonry compressive strength, considering all five performance indices presented in Table 8, already introduced.

4.3. ANN-based closed form equation for the estimation of masonry compressive strength

It is a common practice in machine learning research for researchers to present only part of the details of the predictive models they develop and propose, along with their performance indices. However, without providing all the parameters required to create these models, it becomes impossible to verify their reliability, and even more so, to replicate or build upon these models by other researchers. To illustrate this point, it is worth noting that no proposed ANN model can be reproduced without providing, along with the architecture, the final values of weights and biases.

In light of the above, this subsection presents the closed-form equation Eq. (6) for estimating masonry compressive strength based on the developed and proposed optimal ANN-LM 4–9–1 model. Specifically, the masonry compressive strength (f_{wc}) in relation to the masonry unit compressive strength (f_{bc}), the mortar compressive strength (f_{mc}),

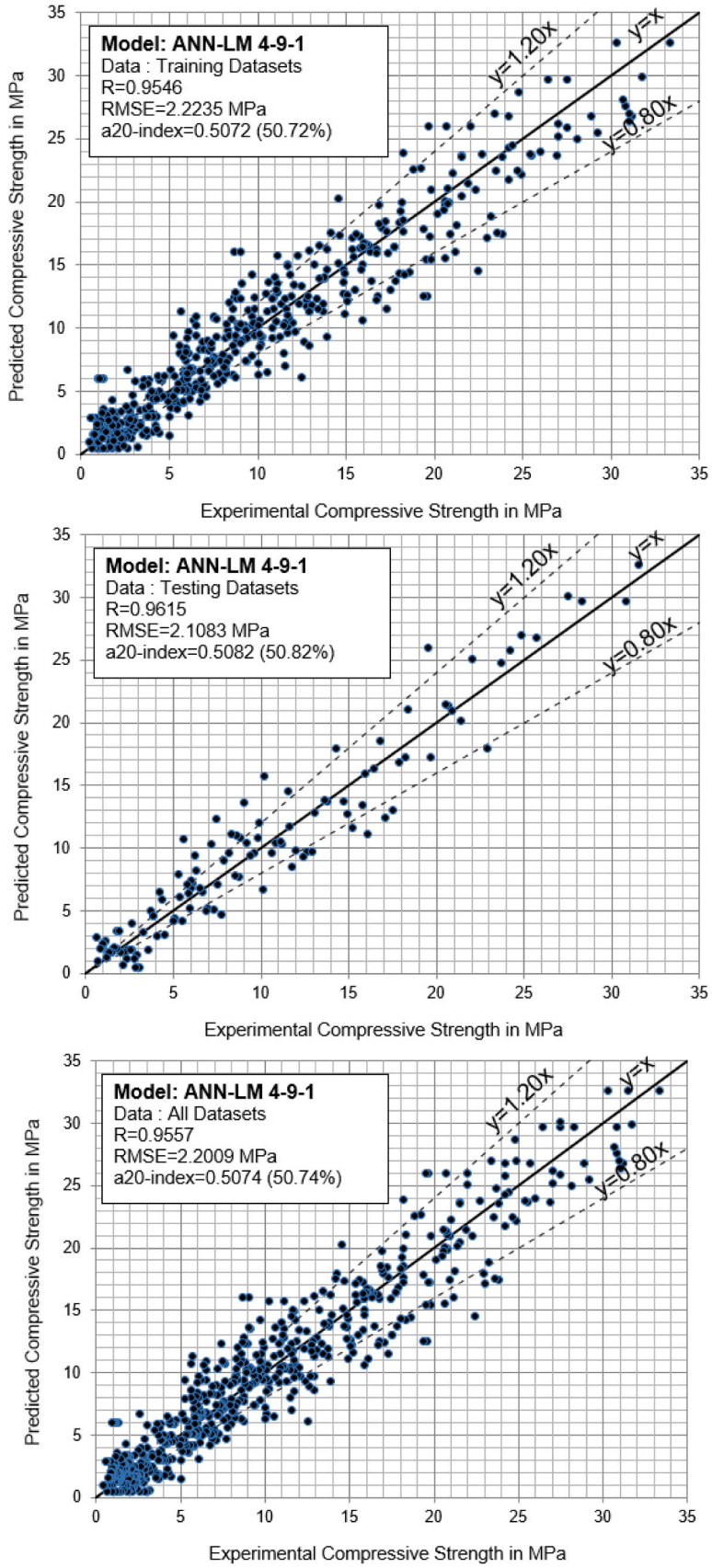

Fig. 4. Experimental ('true') vs Predicted values of the masonry compressive strength for the developed and proposed optimal ANN-LM 4–9–1 model.

Table 9
Final values of weights and biases of the optimal ANN-LM 4–9-1 model.

$[I_W]$ (9 ×4)				$[L_W]^T$ (9 ×1)	$[b_i]$ (9 ×1)	$[b_0]$ (1 ×1)
11.94815	−87.50208	−16.91220	0.08752	−30.40946	−0.78908	63.16957
−0.16434	−0.08828	0.21761	0.09588	−63.74307	−0.10795	
−8.70208	3.29864	7.36559	−15.03860	−1.04069	15.96637	
5.43286	0.23739	1.15692	−0.49509	80.31513	0.55455	
0.79220	1.02951	−3.32502	−26.76595	−1.19873	11.62022	
−1.95824	−1.65733	4.54037	−6.22362	−1.22580	3.17310	
−62.05147	16.63407	−51.35296	41.16826	0.89023	6.06927	
−1.60589	1.32127	79.66294	44.47994	1.28249	−38.00081	
4.35289	0.17715	0.83315	−0.37139	−163.47946	0.94408	

Table 10
Summary of prediction capability of the developed optimal model against the five highest-performing proposals in literature, based on a20-index and testing datasets.

Ranking	Source	Model	Method	Performance Indices				
				a20-index	R^2	RMSE (MPa)	MAPE	VAF
1	This article	ANN-LM 4–9–1	ANNs	0.5082	0.9615	2.1083	0.3391	92.0625
2	Lumantarna et al., [81]	$f_{wc} = 0.75 {f_{bc}}^{0.75} {f_{mc}}^{0.31}$	RG	0.3033	0.7454	6.0370	0.4176	46.8621
3	Engesser [49]	$f_{wc} = \frac{1}{3} f_{bc} + \frac{2}{3} f_{mc}$	RG	0.3033	0.7338	6.5148	0.4295	47.3341
4	Tassios [129]	$f_{wc} = \frac{2}{3} f_{bc} + 0.1 f_{mc}$	RG	0.2951	0.7774	7.9218	0.4099	15.4996
5	Moayedian, Hejazi [94]	$f_{wc} = 0.6 {f_{bc}}^{0.7} {f_{mc}}^{0.4}$	RG	0.2705	0.7876	4.7425	0.4388	61.0820
6	Mann [84]	$f_{wc} = 0.83 {f_{bc}}^{0.66} {f_{mc}}^{0.18}$	RG	0.2377	0.8239	4.7257	0.5028	64.0042

RG: Regression Analysis

the masonry height to thickness ratio (h_w/t_w), and the mortar thickness to masonry unit thickness ratio (t_m/t_b) is given in matrix form by:

$$f_{wc} = 33.05 \times logsig([L_W] \times [\text{radbas}([I_W] \times [IP] + [b_i])] + [b_0]) + 0.45 \quad (6)$$

where [IP] is a 4 × 1 vector with the normalized values of the four input parameters given by Eq. (7):

$$[IP] = \begin{bmatrix} \frac{f_{bc} - 2.30}{72.6} \\ \frac{f_{mc} - 0.30}{31.7} \\ \frac{(h_w/t_w) - 1.15}{7.45} \\ \frac{(t_m/t_b) - 0.01}{0.32} \end{bmatrix} \quad (7)$$

In this equation, logsig is the Log-sigmoid transfer function, and radbas refers to the Radial Basis transfer function. $[I_W]$ is a 9 × 4 containing the weights of the hidden layer, $[L_W]$ is a 1 × 9 vector containing the weights of the output layer, $[b_i]$ is a 9 × 1 vector containing the bias values of the hidden layer, and $[b_0]$ is a 1 × 1 vector containing the bias values of the output layer. All these matrices are provided in Table 9.

The above proposed equation, which is based on the developed and proposed ANN 4–9–1 optimal model, can be integrated into any software and any programming environment. This helps to disprove the widely accepted idea that ANN models are "black boxes", while also making the proposed model a particularly useful tool for researchers, and even more so for practicing engineers.

4.4. Comparison of the developed models and available proposals in the literature

The optimal machine learning model of this study presented in previous sections (ANN-LM 4–9–1) is compared here with available proposals that predict the compressive strength of masonry walls, found in literature. This comparison is performed according to the selected performance indices. A full comparison is provided in the supplementary document entitled *Prediction Performance Comparison*. This comparison is curtailed in Table 10, which summarises the performance of the proposed ANN model and the five highest performing semi-empirical models. The optimal, ANN-LM 4–9–1 model proposed in this study leads to the highest a-20 index which at least 65 % higher, when compared to the remaining studies, indicating an improved performance of the proposed ANN architecture.

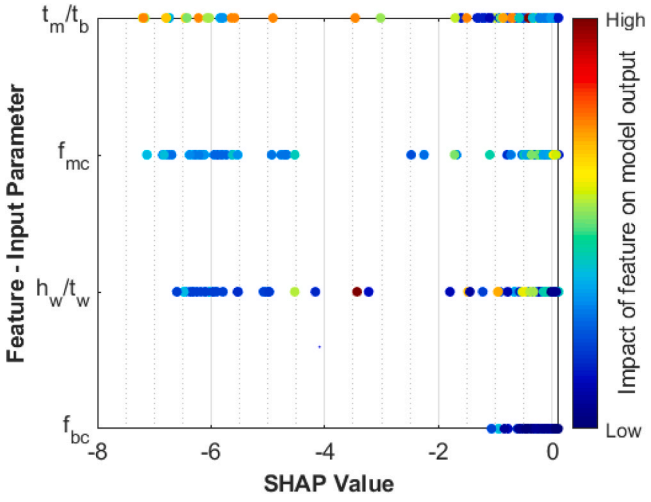

Fig. 5. Assessment of the parameters influencing the masonry compressive strength based on optimal ANN-LM 4–9–1 model and using SHapley Additive exPlanations (SHAP) method: SHAP value for each one dataset of input parameters influencing the masonry compressive strength.

It is worth noticing that the other indices are also significantly improved in comparison with the literature findings, further emphasizing the capacity of the proposed machine learning model to predict the compressive strength of masonry walls. For instance, the R^2 index of the ANN-LM 4–9–1 is equal to 0.9615, while the highest R^2 index

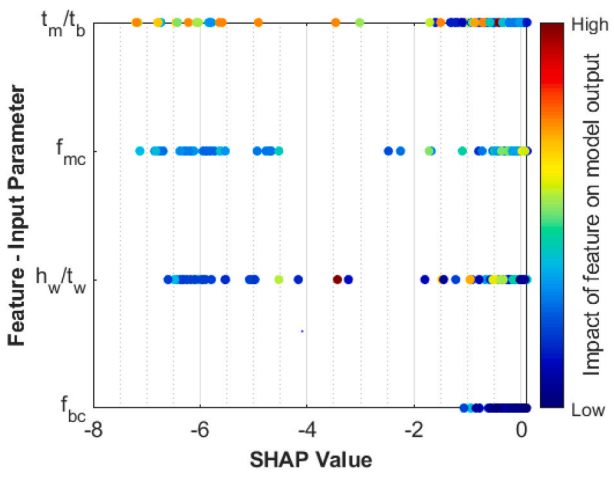

a) All samples; masonry compressive strength up to 33 MPa

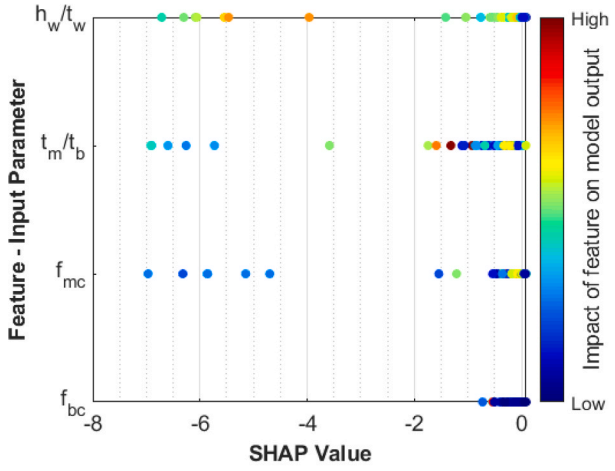

b) Samples with masonry compressive strength up to 15 MPa

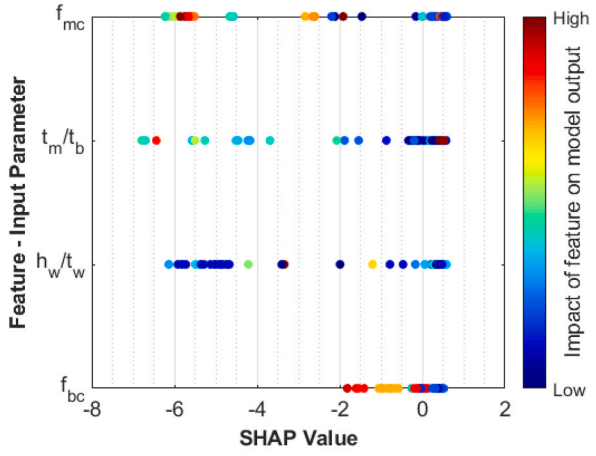

c) Samples with masonry compressive strength greater than 15 MPa

Fig. 6. Assessment of the parameters influencing the masonry compressive strength based on optimal ANN-LM 4–9–1 model and using SHapley Additive exPlanations (SHAP) method.

obtained from literature is 0.8262 [66]. RMSE and MAPE values obtained from this study are also significantly lower when compared to existing literature while the VAF value of this study is the highest among the ones presented in Table 10.

4.5. Assessment of the parameters affecting masonry compressive strength

Aiming to reveal the nature of masonry materials, this subsection seeks to evaluate the parameters that influence the compressive strength of masonry and to rank them based on their impact. For this purpose, the optimal developed ANN-LM 4–9–1 model and the SHapley Additive exPlanations (SHAP) method, recently proposed [31,82], are used to determine the significance of each input parameter on the output parameter. These parameters are then ranked from the most to the least influential.

The resulting average SHAP values for the input parameters are: 0.5574 for t_m/t_b, 0.4952 for f_{mc}, 0.4764 for h_w/t_w and 0.1079 for f_{bc}. Additionally, the SHAP values for each individual sample (dataset) are presented in Fig. 5. Based on these results, it is evident that the most important parameter affecting the compressive strength of masonry is the mortar thickness to masonry unit thickness ratio (t_m/t_b) followed in order by the mortar compressive strength (f_{mc}), the masonry height to thickness ratio (h_w/t_w) and the parameter with the smallest influence, which is the masonry unit compressive strength (f_{bc}).

To further explore the complex behaviour and nature of masonry materials, an analysis was conducted to assess the influence of these four parameters, with a distinction made between whether the masonry is "strong" or "weak," using the compressive strength of 15 MPa as threshold. The results are presented in Fig. 6, both for the entire dataset of 611 experimental samples and for the subsets of "weak" masonry with compressive strength up to 15 MPa (475 samples) and "strong" masonry with compressive strength greater than 15 MPa (136 samples). Based on this analysis, the following observations can be made:

- For the entire dataset of 611 samples, with compressive strength ranging from 0.45 to 33.30 MPa, the critical parameter is the mortar thickness to masonry unit thickness ratio (t_m/t_b),
- For "weak" masonry, the main parameter affecting compressive strength is the masonry height to thickness ratio (h_w/t_w),
- For "strong" masonry, the primary parameter influencing compressive strength is the mortar compressive strength (f_{mc}),
- In all cases, the parameter with the least influence is the masonry unit compressive strength (f_{bc}).

4.6. Mapping and revealing the nature of masonry compressive strength

In this section, using the proposed optimal ANN-LM 4–9–1 model, an attempt will be made to map and reveal the complex nature of masonry through the production of a set of graphs. These graphs will also demonstrate that the well-known and frequently encountered problem of overfitting did not occur during the model's training. Specifically, Fig. 7 depicts the relationship between masonry compressive strength and the compressive strength of the masonry unit for masonry height to thickness ratios of 5.00, 6.00, 7.00, and 8.00 using the optimal ANN-LM 4–9–1 model, with a mortar thickness to masonry unit thickness ratio of 0.10. Additionally, Fig. 8 illustrates the curves of masonry compressive strength versus the compressive strength of mortar for a mortar thickness to masonry unit thickness ratio of 0.10, with mortar unit strength ranging from 10.00 to 70.00 MPa in increments of 10.00 MPa, using the optimal ANN-LM 4–9–1 model.

Based on these mappings, the following points can be made:

- The smoothness of the contours confirms that the proposed computational methodology avoids the overfitting of data, a common issue in the development of prognostic soft computing models. In cases of

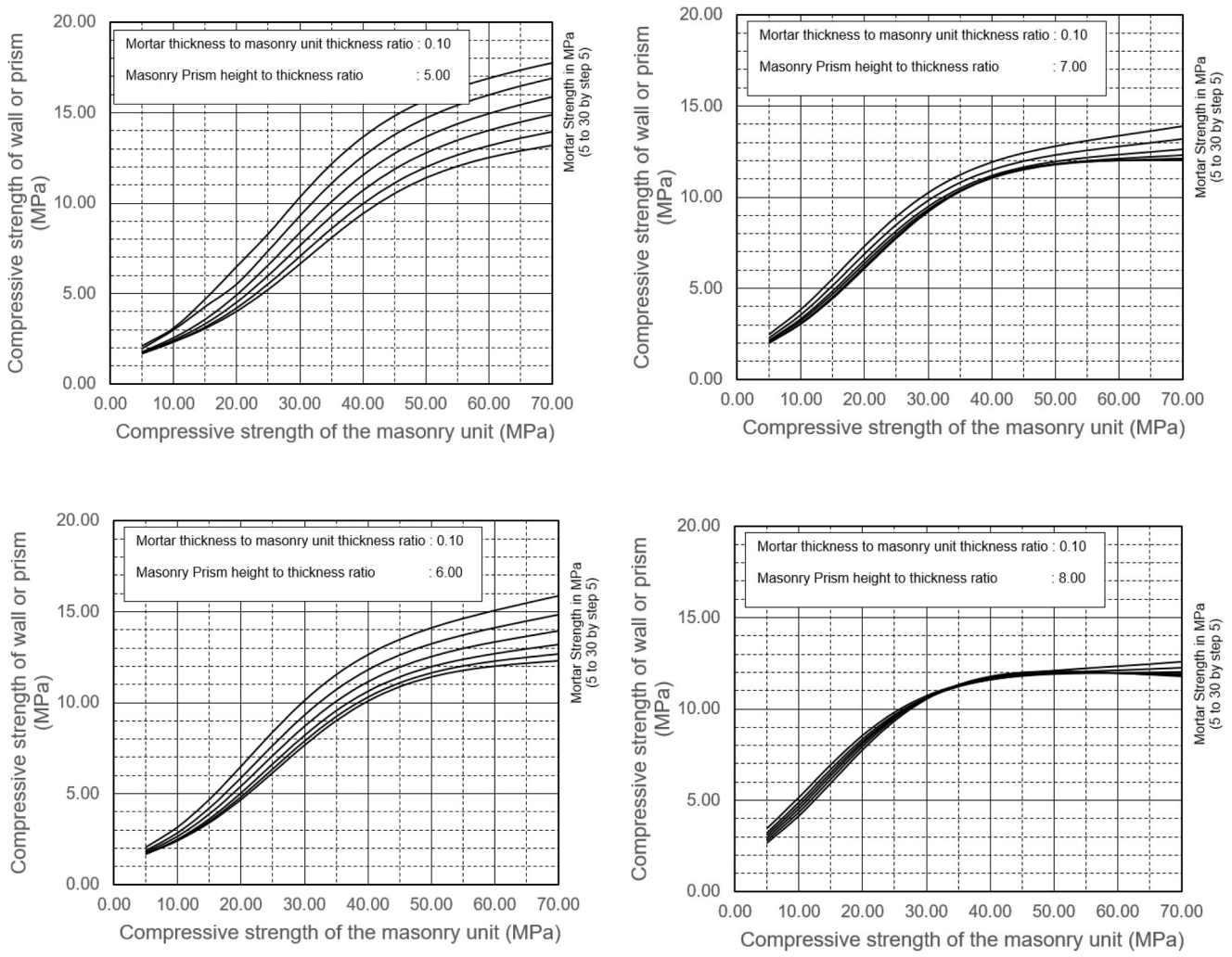

Fig. 7. Masonry compressive strength vs Compressive strength of the masonry unit for mortar thickness to masonry unit thickness ratio 0.10 and masonry height to thickness ratio 5.00, 6.00, 7.00 and 8.00 using the optimal ANN-LM 4–9–1 model.

overfitting, the model may appear to fit very closely to the experimental data used for its training; however, for slightly perturbed data ranges, the predictions become significantly worse,

- The relationship between masonry compressive strength and the compressive strength of the masonry unit is nonlinear, and this nonlinearity becomes particularly pronounced for masonry unit compressive strength values exceeding 20.00 MPa (Fig. 7),
- In contrast, the relationship between masonry compressive strength and mortar strength is linear (Fig. 8),
- According to Fig. 7, for mortar thickness to masonry unit thickness ratio (t_m/t_b) equal to 0.1, an increase of the mortar strength results in increase of the masonry compressive strength. This is more intense for higher compressive strength values of the masonry unit.
- According to Fig. 7, for $t_m/t_b = 0.10$ the compressive strength of masonry becomes less sensitive to f_{mc} for higher values of h_w/t_w (higher slenderness), highlighting the effect of geometric slenderness on the compressive strength of masonry.

5. Limitations and future research

The database used for the development and training of a predictive model defines the model limitations and determines the range of parameter values for which updates are necessary. Specifically, every predictive computational model is valid for input parameter values that fall between the minimum and maximum values defined by the database. Conversely, for parameter values outside these limits, the reliability of the predictions is compromised, as the model has not been trained on such values.

In light of the above, the optimal ANN-LM 4–9–1 model proposed in this study is valid for parameter values within the minimum and maximum ranges specified in Table 6. Additionally, as previously mentioned, the database defines the parameter value ranges that require further research and corresponding updates. These ranges are specifically indicated by the histograms of parameters used for predicting masonry compressive strength, which were presented in Fig. 2. Based on these histograms, the reliability of the proposed model is uncertain for parameter value ranges where the data is insufficient, such as for values of the mortar thickness to masonry unit thickness ratio (t_m/t_b) greater than 0.20, where the number of data points is quite small.

Although the database used in this study is the largest ever compiled and utilized for the development of predictive mathematical models in this context, the authors have set immediate research goals to update it. The aim is to formulate a more reliable computational model for predicting masonry compressive strength, thereby contributing to the design of more reliable and safe masonry structures.

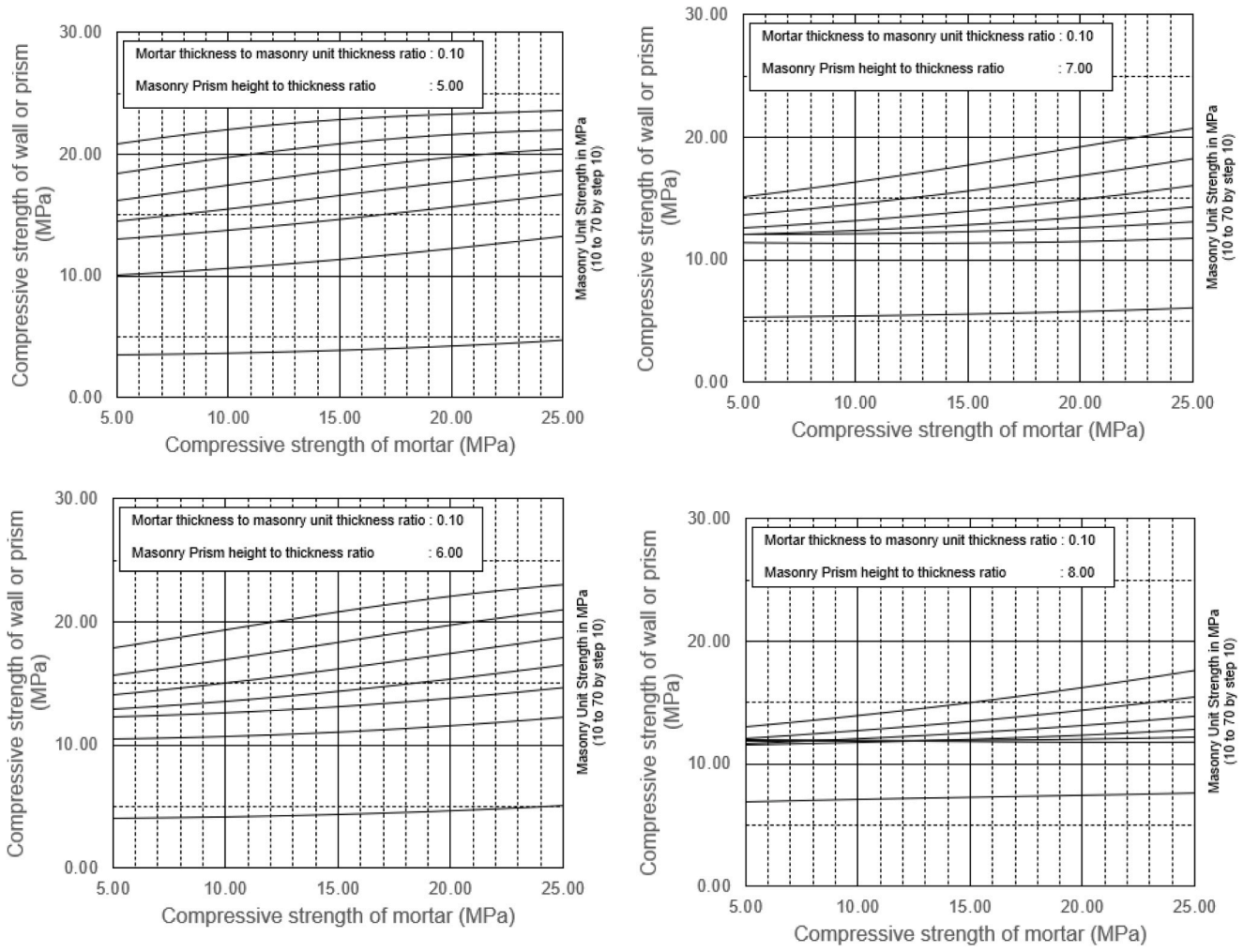

Fig. 8. Masonry compressive strength vs Compressive strength of mortar for mortar thickness to masonry unit thickness ratio 0.10 and masonry unit strength 10.00–70.00 by step 10.00 using the optimal ANN-LM 4–9–1 model.

6. Conclusions

A comprehensive experimental database of 611 data points, collected from 81 experimental campaigns, is developed in this study to formulate an optimal computational model predicting the compressive strength of masonry. Four parameters, namely, the compressive strength of the masonry unit, the compressive strength of the mortar, the masonry height to thickness ratio and the mortar thickness to masonry unit thickness ratio are considered as input in this database, while one output parameter, the compressive strength of masonry is used.

Back Propagation Neural Networks (BPNN) models are then developed and trained to predict the compressive strength of masonry using four different optimization algorithms, namely, the Levenberg-Marquardt algorithm, the Broyden–Fletcher–Goldfarb–Shanno algorithm, the Particle Swarm Optimization algorithm, and the Imperialist Competitive Algorithm (ICA). To identify the optimal computational scheme that can more effectively predict the compressive strength of masonry, combinations for architectures have been tested and ranked based on their performance, adopting different numbers of neurons per hidden layer and different transfer functions.

The investigation leads to an optimal ANN model, optimized using the Levenberg-Marquardt algorithm, consisting of a structure with 9 neurons in the hidden layer, and employing the Minmax normalization technique in the range [0.00–1.00]. The Radial Basis (RB) transfer function is used in the hidden layer, while the Log-sigmoid transfer function is utilized in the output layer of this optimal model.

The capacity of the optimal machine learning model of this study to predict the compressive strength of masonry is highlighted, by a comparison with available literature proposals. Within this comparison, all performance indices obtained from the proposed model are significantly improved in comparison with the literature findings.

Using the optimal developed model, the contribution of each input parameter on the prediction of the compressive strength of masonry is evaluated, by adopting the SHapley Additive exPlanations (SHAP) method. It is shown that the most important parameter affecting the compressive strength of masonry is the mortar thickness to masonry unit thickness ratio followed in order by the mortar compressive strength, the masonry height to thickness ratio and the parameter with the smallest influence, which is the masonry unit compressive strength. However, when the investigation differentiates between masonry compressive strength values above 15 MPa (strong) or below 15 MPa (weak), a different outcome is obtained. Thus, for weak masonry, the main parameter affecting compressive strength is the masonry height to thickness ratio, while for strong masonry, the primary parameter influencing compressive strength is the mortar compressive strength.

Finally, the optimal computational model is used to further investigate and evaluate the nature of the compressive strength of masonry. Based on this investigation it is concluded that the relationship between the compressive strength of the masonry wall/prism and the compressive strength of the masonry unit is nonlinear. It is also shown that for higher slenderness of the masonry walls, increasing the mortar strength has less or almost no influence on the masonry compressive strength.

The study can be extended by further enriching the developed database, covering potential input parameters areas with less dense representation, such as units and mortar with compressive strength higher than 20 MPa. Additionally, the dataset can be expanded with the inclusion of typologies such as stone masonries in greater numbers.

CRediT authorship contribution statement

Amin Mohebkhah: Writing – review & editing, Writing – original draft, Visualization, Validation, Methodology, Investigation. **Anastasios Drougkas:** Writing – review & editing, Writing – original draft, Visualization, Validation, Methodology, Investigation. **Gabriele Milani:** Writing – review & editing, Writing – original draft, Visualization, Validation, Methodology, Investigation. **Liborio Cavaleri:** Writing – review & editing, Writing – original draft, Visualization, Validation, Methodology, Investigation. **Antonio Formisano:** Writing – review & editing, Writing – original draft, Visualization, Validation, Methodology, Investigation. **Panagiotis G. Asteris:** Writing – review & editing, Writing – original draft, Supervision, Software, Methodology, Investigation, Conceptualization. **Georgios A. Drosopoulos:** Writing – review & editing, Writing – original draft, Visualization, Validation, Methodology, Investigation. **Paulo B. Lourenço:** Writing – review & editing, Writing – original draft, Visualization, Validation, Methodology, Investigation.

Supplementary material

The *Parameters of ANNs*, the *Top 20 ANN Architectures* and *Comparison with Semi-Empirical Models* are included as supplementary material to this paper.

Declaration of Competing Interest

The authors declare that they have no known competing financial interests or personal relationships that could have appeared to influence the work reported in this paper.

Appendix A. Supporting information

Supplementary data associated with this article can be found in the online version at doi:10.1016/j.istruc.2025.109189.

Data Availability

Data will be made available on request.

References

[1] AbdelRahman B, Galal K. Influence of pre-wetting, non-shrink grout, and scaling on the compressive strength of grouted concrete masonry prisms. Constr Build Mater 2020;241:117985.

[2] ACI 530.1-02/ASCE 6-02/TMS 602-22, n.d. Specification for Masonry Structures, Reported by the Masonry Standards Joint Committee (MSJC).

[3] Alavi AH, Gandomi AH. Energy-based numerical models for assessment of soil liquefaction. Geosci Front 2012;3(4):541–55.

[4] Aliu AA, Ariff NRM, Ametefe DS, John D. Automatic classification and isolation of cracks on masonry surfaces using deep transfer learning and semantic segmentation. J Build Rehabil 2023;8:28. https://doi.org/10.1007/s41024-023-00274-6.

[5] Alkayem NF, Shen L, Mayya A, Asteris PG, Ronghua F, Di Luzio G, Strauss A, Cao M. Prediction of concrete and FRC properties at high temperature using machine and deep learning: a review of recent advances and future perspectives. J Build Eng 2023;83:108369.

[6] Andolfato RP, Camacho JS, Ramalho MA. Brazilian results on structural masonry concrete blocks. MJ 2007;104:33–9. https://doi.org/10.14359/18492.

[7] Apostolopoulou M, Armaghani DJ, Bakolas A, Douvika MG, Moropoulou A, Asteris PG. Compressive strength of natural hydraulic lime mortars using soft computing techniques. Procedia Struct Integr 2019;17:914–23.

[8] Armaghani DJ, Asteris PG. A comparative study of ANN and ANFIS models for the prediction of cement-based mortar materials compressive strength. Neural Comput Appl 2020;33:4501–32. https://doi.org/10.1007/s00521-020-05244-4.

[9] AS Committee 3700-2018, Masonry structures. Australian Standard Association, Sydney;2018.

[10] Asteris PG, Antoniou ST, Sophianopoulos DS, Chrysostomou CZ. Mathematical Macromodeling of Infilled Frames: State of the Art. J Struct Eng 2011;137:1508–17. https://doi.org/10.1061/(ASCE)ST.1943-541X.0000384.

[11] Asteris PG, Argyropoulos I, Cavaleri L, Rodrigues H, Varum H, Thomas J, Lourenço PB. Masonry Compressive Strength Prediction using Artificial Neural Networks. Presented at the International Conference on Transdisciplinary Multispectral Modeling and Cooperation for the Preservation of Cultural Heritage. Cham, Switzerland, Athens, Greece: Springer; 2018. p. 200–24.

[12] Asteris PG, Lourenço PB, Hajihassani M, Adami C-EN, Lemonis ME, Skentou AD, Marques R, Nguyen H, Rodrigues H, Varum H. Soft computing-based models for the prediction of masonry compressive strength. Eng Struct 2021;248:113276. https://doi.org/10.1016/j.engstruct.2021.113276.

[13] Asteris PG, Mokos VG. Concrete Compressive Strength using Artificial Neural Networks. Neural Comput Appl 2019. https://doi.org/10.1007/s00521-019-04663-2.

[14] Asteris PG, Plevris V. Anisotropic masonry failure criterion using artificial neural networks. Neural Comput Appl. 2017;28:2207–29. https://doi.org/10.1007/s00521-016-2181-3.

[15] ASTM C 1552-23, Practice for capping concrete masonry units, related units and masonry prisms for compression testing. West Conshohocken, USA; 2023.

[16] ASTM C1314-22. Standard Test Method for Compressive Strength of Masonry Prisms. West Conshohocken, PA: ASTM International; 2022.

[17] ASTM C270-24, Standard Specification for Mortar for Unit Masonry. USA; 2024.

[18] ASTM E 122-17, Standard practice for calculating sample size to estimate, with specified precision, the average for a characteristic of a lot or process. West Conshohocken, USA; 2017.

[19] Atashpaz-Gargari E, Lucas C. Imperialist competitive algorithm: An algorithm for optimization inspired by imperialistic competition. 2007 IEEE Congress on Evolutionary Computation, 2007. CEC; 2007. p. 4661–7. 4425083.

[20] Bakhteri J, Sambasivam S. Mechanical behaviour of structural brick masonry: an experimental evaluation. Proc 5th Asia - Pac Struct Eng Constr Conf, Malays 2003:305–17.

[21] Balasubramanian SR, Maheswari D, Cynthia A, Rao KB, Prasad MA, Goswami R, Sivakumar P. Experimental determination of statistical parameters associated with uniaxial compression behaviour of brick masonry. Curr Sci 2015;109(11):2094–102.

[22] Barbosa CS, Lourenço PB, Hanai JB. On the compressive strength prediction for concrete masonry prisms. Mater Struct 2010;43:331–44. https://doi.org/10.1617/s11527-009-9492-0.

[23] Basha SH, Kaushik HB. Evaluation of nonlinear material properties of fly ash brick masonry under compression and shear. J Mater Civ Eng 2015;27:04014227. https://doi.org/10.1061/(ASCE)MT.1943-5533.0001188.

[24] Bennett RM, Boyd KA, Flanagan RD. Compressive Properties of Structural Clay Tile Prisms. J Struct Eng 1997;123:920–6. https://doi.org/10.1061/(ASCE)0733-9445(1997)123:7(920).

[25] Binda L, Fontana A, Frigerio G. Mechanical behaviour of brick masonries derived from unit and mortar characteristics. Presented at the 8th International Brick and Block Masonry Conference. Dublin Repub Irel 1988;1:205–16.

[26] Boffill Y, Blanco H, Lombillo I, Villegas L. Assessment of historic brickwork under compression and comparison with available equations. Constr Build Mater 2019;207:258–72. https://doi.org/10.1016/j.conbuildmat.2019.02.083.

[27] Bosiljkov V. Experimental and numerical research on the influence of the modified mortars on the mechanical properties of the brick masonry, PhD Thesis. Slovenia: University of Ljubljana; 2000.

[28] Brencich A, Gambarotta L. Mechanical response of solid clay brickwork under eccentric loading. Part I: Unreinforced masonry. Mater Struct 2005;38:257–66.

[29] Bröcker O. Die auswertung von tragfähigkeitsversuchen an gemauerten wänden. Betonstein-Zeitung; 1963. p. 19–21.

[30] Carvalho M.A.B., 2015. Development and validation of a constructive solution in BTC, Master Thesis, UniMinho (in Portuguese).

[31] Cavaleri L, Barkhordari MS, Repapis CC, Armaghani DJ, Ulrikh DV, Asteris PG. Convolution-based ensemble learning algorithms to estimate the bond strength of the corroded reinforced concrete. Constr Build Mater 2022;359. https://doi.org/10.1016/j.conbuildmat.2022.129504.

[32] Cavaleri L, Di Trapani F, Macaluso G, Papia M. Attendibilità dei modelli per la valutazione dei moduli elastici delle murature suggeriti dalle norme tecniche. Ing sismica 2012;29(1):38–59.

[33] Cavaleri L, Di Trapani F. Cyclic response of masonry infilled RC frames: Experimental results and simplified modeling. Soil Dyn Earthq Eng 2014;65:224–42.

[34] Cavaleri L, Papia M, Macaluso G, Di Trapani F, Colajanni P. Definition of diagonal Poisson's ratio and elastic modulus for infill masonry walls. Mater Struct 2014;47(1-2):239–62.

[35] Cheema TS, Klinger RE. Compressive Strength of Concrete Masonry Prisms. JP 1986;83:88–97. https://doi.org/10.14359/1752.

[36] Christy CF, Tensing D, Shanthi RM. Experimental study on axial compressive strength and elastic modulus of the clay and fly ash brick masonry. J Civ Eng Constr Technol 2013;4:134–41.

[37] CTE, 2008. Spanish Technical Building Code.

[38] Cuomo M, Badalà A. Problematiche metodologiche relative alla determinazione sperimentale delle proprietà meccaniche dei materiali murari e dei loro componenti. La Prot Del Patrim Cult–la Quest Sismica 1997:657–83.

[39] Dais D, Bal İE, Smyrou E, Sarhosis V. Automatic crack classification and segmentation on masonry surfaces using convolutional neural networks and

transfer learning. Autom Constr 2021;125:103606. https://doi.org/10.1016/j.autcon.2021.103606.
[40] Dayaratnam P. Brick and Reinforced Brick Structures. Oxford & IBH; 1987.
[41] Drosopoulos GA, Stavroulakis GE. Nonlinear mechanics for composite heterogeneous structures. Boca Raton London New York: CRC Press, Taylor & Francis Group; 2022.
[42] Drougkas A, Roca P, Molins C. Compressive strength and elasticity of pure lime mortar masonry. Mater Struct 2016;49:983–99. https://doi.org/10.1617/s11527-015-0553-2.
[43] Drysdale RG, Hamid AA. Behavior of Concrete Block Masonry Under Axial Compression. JP 1979;76:707–22. https://doi.org/10.14359/6965.
[44] Dymiotis C, Gutlederer BM. Allowing for uncertainties in the modelling of masonry compressive strength. Constr Build Mater 2002;16:443–52. https://doi.org/10.1016/S0950-0618(02)00108-3.
[45] EN 1015-11:2019 - Methods of test for mortar for masonary - Part 11: Determination of flexural and compressive strength of hardened mortar. European Committee for Standardization, Brussels.
[46] EN 1052-1. Methods of test for masonry - Part 1: Determination of compressive strength. Brussels: European Committee for Standardization; 1998.
[47] EN 1996-1-1. Eurocode 6: Design of masonry structures-Part 1-1: General rules for reinforced and unreinforced masonry structures. Brussels: European Committee for Standardization; 2005.
[48] EN 772-1:2011 - Methods of test for masonry units – Part 1: Determination of compressive strength. European Committee for Standardization, Brussels.
[49] Engesser F. Über weitgespannte Wölbbrücken (in German). Z FüR Archit und Ing 1907;53:403–40.
[50] Fakharian P, Rezazadeh Eidgahee D, Akbari M, Jahangir H, Ali Taeb A. Compressive strength prediction of hollow concrete masonry blocks using artificial intelligence algorithms. Structures 2023;47:1790–802. https://doi.org/10.1016/j.istruc.2022.12.007.
[51] Fletcher R. Practical methods of optimization. New York: John Wiley & Sons; 1975.
[52] Fonseca FS, Fortes ES, Parsekian GA, Camacho JS. Compressive strength of high-strength concrete masonry grouted prisms. Constr Build Mater 2019;202:861–76.
[53] Fortes ES, Parsekian GA, Fonseca FS. Relationship between the Compressive Strength of Concrete Masonry and the Compressive Strength of Concrete Masonry Units. J Mater Civ Eng 2015;27:04014238. https://doi.org/10.1061/(ASCE)MT.1943-5533.0001204.
[54] Francis AJ, Horman CB, Jerems LE. The effect of joint thickness and other factors on the compressive strength of brickwork, 2nd International brick masonry conference. Stoke-on-Trent 1970:31–7.
[55] Furtado A, Rodrigues H, Arêde A, et al. Mechanical properties characterization of different types of masonry infill walls. Front Struct Civ Eng 2020;14:411–34.
[56] Furtado A, Rodrigues H, Arêde A, Varum H. Experimental evaluation of out-of-plane capacity of masonry infill walls. Eng Struct 2016;111:48–63.
[57] Garzón-Roca J, Marco CO, Adam JM. Compressive strength of masonry made of clay bricks and cement mortar: Estimation based on Neural Networks and Fuzzy Logic. Eng Struct 2013;48:21–7. https://doi.org/10.1016/j.engstruct.2012.09.029.
[58] Gautam D, Adhikari R, Olafsson S, Rupakhety R. "Damage description, material characterization, retrofitting, and dynamic identification of a complex neoclassical monument affected by the 2015 Gorkha, Nepal earthquake". J Build Eng 2023;80:108152.
[59] Gayed M., Korany Y., Sturgeon G. (2012). Examination of the prescribed concrete block masonry compressive strength in the Canadian masonry design standard, CSA S304. 1-04 15th International Brick and Block Masonry Conference, Florianopolis, Brazil, 2012.
[60] Gholami M, Gholami A. Prediction of compressive strength of masonry structures: Integrating three optimized models by virtue of committee machine. Structures 2022;44:1127–37. https://doi.org/10.1016/j.istruc.2022.08.079.
[61] Gholami M, Ranjbargol M, Yousefzadeh R, Ghorbani Z. Integrating three smart predictive models using a power-law committee machine for the prediction of compressive strength in masonry made of clay bricks and cement mortar. Structures 2023;55:951–64. https://doi.org/10.1016/j.istruc.2023.06.058.
[62] Graus S, Vasconcelos G, Palha C. Experimental characterization of the deterioration of masonry materials due to wet and dry and salt crystallization cycles. In: Aguilar R, Torrealva D, Moreira S, Pando MA, Ramos LF, editors. Structural Analysis of Historical Constructions. RILEM Bookseries, 18. Cham: Springer; 2019.
[63] Gregoire Y. Compressive strength of masonry according to Eurocode 6: a contribution to the study of the influence of shape factors. Mason Int, MI J Artic 2007;20.
[64] Gumaste KS, Nanjunda Rao KS, Venkatarama Reddy BV, Jagadish KS. Strength and elasticity of brick masonry prisms and wallettes under compression. Mater Struct 2007;40:241–53. https://doi.org/10.1617/s11527-006-9141-9.
[65] Haach V, Vasconcelos G, Lourenço PB. Experimental analysis of reinforced concrete block masonry walls subjected to in-plane cyclic loading. J Struct Eng 2010;136(4):452–62.
[66] Hendry AW, Malek MH. Characteristic compressive strength of brickwork walls from collected test results. Mason Int 1986;7:15–24.
[67] Hossain MM, Ali SS, Rahman MA. Properties of masonry constituents. J Civ Eng 1997;25(2):135–55.
[68] Ip, F. (1999), "Compressive Strength and Modulus of Elasticity of Masonry Prisms", Master of Engineering Thesis, Carleton University, Ottawa.
[69] Kaushik HB, Rai DC, Jain SK. Stress-Strain Characteristics of Clay Brick Masonry under Uniaxial Compression. J Mater Civ Eng 2007;19:728–39. https://doi.org/10.1061/(ASCE)0899-1561(2007)19:9(728).
[70] Kennedy J, Eberhart R. Particle swarm optimization. IEEE Int Conf Neural Netw - Conf Proc 1995;4:1942–8.
[71] Khalaf FM. Factors influencing compressive strength of concrete masonry prisms. Mag Concr Res 1996;48:95–101. https://doi.org/10.1680/macr.1996.48.175.95.
[72] Khalaf FM, Hendry AW, Fairbairn DR. Study of the Compressive Strength of Blockwork Masonry. SJ 1994;91:367–75. https://doi.org/10.14359/4139.
[73] Khan NA, Aloisio A, Monti G, Nuti C, Briseghella B. Experimental characterization and empirical strength prediction of Pakistani brick masonry walls. J Build Eng 2023;71:106451. https://doi.org/10.1016/j.jobe.2023.106451.
[74] Köksal HO, Karakoç C, Yildirim H. Compression behavior and failure mechanisms of concrete masonry prisms. J Mater Civ Eng 2005;17:107–15. https://doi.org/10.1061/(ASCE)0899-1561(2005)17:1(107).
[75] Kumavat HR. An experimental investigation of mechanical properties in clay brick masonry by partial replacement of fine aggregate with clay brick waste. J Inst Eng India Ser A 2016;97:199–204. https://doi.org/10.1007/s40030-016-0178-7.
[76] Lourakis MIA. A brief description of the Levenberg-Marquardt algorithm implemented by levmar, Hellas (FORTH. Institute of Computer Science Foundation for Research and Technology; 2005. ⟨http://www.ics.forth.gr/~lourakis/levmar/levmar⟩.
[77] Lourenço PB. Computations on historic masonry structures. Prog Struct Eng Maths 2002;4:301–19. https://doi.org/10.1002/pse.120.
[78] Lourenço PB, Avila L, Vasconcelos G, et al. Experimental investigation on the seismic performance of masonry buildings using shaking table testing. Bull Earthq Eng 2013;11:1157–90.
[79] Lourenço PB, Vasconcelos G, Medeiros P, Gouveia J. Vertically perforated clay brick masonry for loadbearing and non-loadbearing masonry walls. Constr Build Mater 2010;24(11):2317–30.
[80] Loverdos D, Sarhosis V. Geometrical digital twins of masonry structures for documentation and structural assessment using machine learning. Eng Struct 2023;275:115256. https://doi.org/10.1016/j.engstruct.2022.115256.
[81] Lumantarna R, Biggs DT, Ingham JM. Uniaxial compressive strength and stiffness of field-extracted and laboratory-constructed masonry prisms. J Mater Civ Eng 2014;26:567–75. https://doi.org/10.1061/(ASCE)MT.1943-5533.0000731.
[82] Lundberg SM, Lee S-I. A unified approach to interpreting model predictions. : Proc Proc 31st Int Conf Neural Inf Process Syst 2017;2017:4768–77.
[83] Machado J., Lübeck A., Mohamad G., Fonseca F., Santos Neto A., Compressive strength of masonry prisms under compression according to Eurocode 6 - EN 1996-1-1 (2005), Proceedings of the 13th North American Masonry Conference, Salt Lake City; 2019.
[84] Mann W. Statistical evaluation of tests on masonry by potential functions. Proc Sixth Int Brick Mason Conf Rome, Italy 1982:86–98.
[85] Martins ROG, Nalon GH, Alvarenga RSS, Pedroti LG, Ribeiro JCL. Influence of blocks and grout on compressive strength and stiffness of concrete masonry prisms. Constr Build Mater 2018;182:233–41.
[86] Mauro A. Long term effects of masonry walls. Italy: University of Roma; 2008.
[87] McNary W, Abrams D. Mechanics of masonry in compression. J Struct Eng 1985;111(4):857–70.
[88] Medeiros P, Vasconcelos G, Lourenço PB, Gouveia J. Numerical modelling of non-confined and confined masonry walls. Constr Build Mater 2013;41:968–76.
[89] Milani G, Lourenço PB, Tralli A. Homogenised limit analysis of masonry walls, Part I: failure surfaces. Comput Struct 2006;84:166–80. https://doi.org/10.1016/j.compstruc.2005.09.005.
[90] Mishra M, Bhatia AS, Maity D. Support vector machine for determining the compressive strength of brick-mortar masonry using NDT data fusion (case study: Kharagpur, India). SN Appl Sci 2019;1:564. https://doi.org/10.1007/s42452-019-0590-5.
[91] Mishra M, Bhatia AS, Maity D. Predicting the compressive strength of unreinforced brick masonry using machine learning techniques validated on a case study of a museum through nondestructive testing. J Civ Struct Health Monit 2020;10:389–403. https://doi.org/10.1007/s13349-020-00391-7.
[92] Mishra M, Bhatia AS, Maity D. A comparative study of regression, neural network and neuro-fuzzy inference system for determining the compressive strength of brick–mortar masonry by fusing nondestructive testing data. Eng Comput 2021;37:77–91. https://doi.org/10.1007/s00366-019-00810-4.
[93] Mishra C., Yamaguchi K., Endo Y., Hanazato T., Mechanical Properties of Components of Nepalese Historical Masonry Buildings", Proceedings of International Exchange and Innovation Conference on Engineering & Sciences (IEICES) 4;2018.
[94] Moayedian SM, Hejazi M. Estimating the modulus of elasticity and the compressive strength of brick, mortar and masonry at different scales. Structures 2024;61:106116. https://doi.org/10.1016/j.istruc.2024.106116.
[95] Mohamad G., Comportamento mecanico na ruptura de prismas de blocos de concreto., Master Thesis, Univeridade Federal de Santa Catarina, Florianópolis; 1998.
[96] Mohamad G, Lourenço PB, Roman HR. Mechanics of hollow concrete block masonry prisms under compression: review and prospects. Cem Concr Compos 2007;29(3):181–92.
[97] Mohamad G., Lourenço P.B., Roman H.R., Mechanical behavior of concrete block masonry - Influence of vertical joint, 2011, 11th NAMC, Mineapolis, USA. (electronic source); 2011.

[98] Mohebkhah A. A nonlinear-seismic model for brick-masonry-infill panels with openings in steel frames, Ph.D. thesis. Tehran (Iran): Tarbiat Modares University; 2007.
[99] Motsa SM, Stavroulakis GE, Drosopoulos GA. A data-driven, machine learning scheme used to predict the structural response of masonry arches. Eng Struct 2023;296:116912. https://doi.org/10.1016/j.engstruct.2023.116912.
[100] MSJC (Masonry Standards Joint Committee), 2013. Building Code Requirements and Specification for Masonry Structures. TMS 402/ACI 530/ASCE 5 and TMS 602/ACI 530.1/ASCE 6.
[101] Muñoz R, Lourenço P, Moreira S. Experimental results on mechanical behaviour of metal anchors in historic stone masonry Construction and Building Materials 2018;163:643–55.
[102] Nagarajan S, Viswanathan S, Ravi V. Experimental approach to investigate the behaviour of brick masonry for different mortar ratios. Proc Int Conf Adv Eng Technol, Singap, March, 2014 2014:586–92.
[103] Nalon GH, Santos CFR, Pedroti LG, Ribeiro JCL, Veríssimo GDS, Ferreira FA. Strength and failure mechanisms of masonry prisms under compression, flexure and shear: Components' mechanical properties as design constraints. J Build Eng 2020;28:101038. https://doi.org/10.1016/j.jobe.2019.101038.
[104] National Concrete Masonry Association (2012). Recalibration of the Unit Strength Method for Verifying Compliance with the Specified Compressive Strength of Concrete Masonry.
[105] Nwofor TC. Experimental determination of the mechanical properties of clay brick masonry. Can J Environ Constr Civil Eng 2012;3(3).
[106] Olatunji TM, Warwaruk J, Longworth J. Behavior and strength of masonry wall/slab joints. Struct Eng Rep 1986:139.
[107] Oliveira J.V. (2014). Mechanical behavior of compressed earth blocks stabilized with alkaline activation. Master Thesis, University of Minho (in Portuguese).
[108] Padalu PKVR, Singh Y. Variation in compressive properties of Indian brick masonry and its assessment using empirical models. Structures 2021;33:1734–53. https://doi.org/10.1016/j.istruc.2021.05.063.
[109] Padalu PKVR, Singh Y, Das S. Uni-axial monotonic compresssive properties of brick masonry in India. Procedings 10th Int Mason Conf (IMC), Pap ID: 639, 1st Ed 2018:1639–55. July 9-11, Milan, Italy.
[110] Radovanović Ž, Sindjic-Grebovic R, Dimovski S, Serdar N, Vatin N, Murgul V. Testing of the mechanical properties of masonry walls – determination of compressive strength. Appl Mech Mater 2015;725-726:410–8.
[111] Ramamurthy K, Sathish V, Ambalavanan R. Compressive Strength Prediction of Hollow Concrete Block Masonry Prisms. SJ 2000;97:61–7. https://doi.org/10.14359/834.
[112] Raposo P, Furtado A, Arêde A, Varum H, Rodrigues H. Mechanical characterization of concrete block used on infill masonry panels. Int J Struct Integr 2018;9(3):281–95.
[113] Ravula MB, Subramaniam KVL. Experimental investigation of compressive failure in masonry brick assemblages made with soft brick. Mater Struct 2017;50:19. https://doi.org/10.1617/s11527-016-0926-1.
[114] Reddy BV, Vyas CVU. Influence of shear bond strength on compressive strength and stress-strain characteristics of masonry. Mater Struct 2008;41(10):1697–712.
[115] Redmond TB, Allen MH. Compressive strength of composite brick and concrete masonry walls. Mason Present Phila ASTM 1975:195–232.
[116] Roberts JJ. The effect of different test procedures upon the indicated strength of concrete blocks in compression. Mag Concr Res 1973;(83):87–98.
[117] Sandeep MV, Renukadevi S, Manjunath S. Behavior of hollow concrete block masonry prism under compression-An experimental and analytical approach. Int J Res Eng Technol (Electron Source) 2013.
[118] Sarhat SR, Sherwood EG. The prediction of compressive strength of ungrouted hollow concrete block masonry. Constr Build Mater 2014;58:111–21. https://doi.org/10.1016/j.conbuildmat.2014.01.025.
[119] Sathiparan N, Jeyananthan P. Prediction of masonry prism strength using machine learning technique: effect of dimension and strength parameters. Mater Today Commun 2023;35:106282. https://doi.org/10.1016/j.mtcomm.2023.106282.
[120] Sathiparan N, Rumeshkumar U. Effect of moisture condition on mechanical behavior of low strength brick masonry. J Build Eng 2018;17:23–31.
[121] Segura J, Pelà L, Roca P. Monotonic and cyclic testing of clay brick and lime mortar masonry in compression. Constr Build Mater 2018;193:453–66.
[122] Self, M.W. (1974), "The structural properties of load-bearing concrete masonry" EIES Proj D-622.
[123] Sharafati A, Haji Seyed Asadollah SB, Al-Ansari N. Application of bagging ensemble model for predicting compressive strength of hollow concrete masonry prism. Ain Shams Eng J 2021;12:3521–30. https://doi.org/10.1016/j.asej.2021.03.028.
[124] Shivaraj Kumar HY, Renuka Devi MV, Sandeep, Manjunath S, Somanath MB. Effect of prism height on strength of reinforced hollow concrete block masonry. Int J Res Eng Technol 2014;03(06) (electronic source).
[125] Singh SB, Munjal P. Bond strength and compressive stress-strain characteristics of brick masonry. J Build Eng 2017;9:10–6.
[126] Skentou AD, Bardhan A, Mamou A, Lemonis ME, Kumar G, Samui P, Armaghani DJ, Asteris PG. Closed-form equation for estimating unconfined compressive strength of granite from three non-destructive tests using soft computing models. Rock Mech Rock Eng 2023;56(2023):487–514. https://doi.org/10.1007/s00603-022-03046-9.
[127] Soundar Rajan M, Jegatheeswaran D. Prediction of autoclaved aerated cement block masonry prism strength under compression using machine learning tools. Matéria (Rio J 2024;29(1):e20230247.
[128] Standoli G, Salachoris GP, Masciotta MG, Clementi F. Modal-based FE model updating via genetic algorithms: Exploiting artificial intelligence to build realistic numerical models of historical structures. Constr Build Mater 2021;303:124393. https://doi.org/10.1016/j.conbuildmat.2021.124393.
[129] Tassios TP. Meccanica delle Murature. Napoli: Liguori Editore; 1988.
[130] Tassios T.P., Chronopoulos M.P., A seismic dimensioning of interventions (repairs/strengthening) on lowstrength masonry building. Presented at the Middle East and Mediterranean Regional Conference on Earthen and low-strength masonry buildings in seismic areas, Ankara, Turkey; 1986.
[131] Thaickavil NN, Thomas J. Behaviour and strength assessment of masonry prisms. Case Stud Constr Mater 2018;8:23–38. https://doi.org/10.1016/j.cscm.2017.12.007.
[132] Thamboo JA. Development of Thin Layer Mortared Concrete Masonry (Ph.D. Dissertation). Brisbane: Queensland University of Technology; 2014.
[133] Thamboo JA. Material characterisation of thin layer mortared clay masonry. Constr Build Mater 2020;230:116932.
[134] Thamboo JA, Dhanasekar M. Correlation between the performance of solid masonry prisms and wallettes under compression. J Build Eng 2019;22:429–38. https://doi.org/10.1016/j.jobe.2019.01.007.
[135] Valero E, Forster A, Bosché F, Hyslop E, Wilson L, Turmel A. Automated defect detection and classification in ashlar masonry walls using machine learning. Autom Constr 2019;106:102846. https://doi.org/10.1016/j.autcon.2019.102846.
[136] Vermeltfoort AT. Compression properties of masonry and its components. Proc 10th Int Brick Block Mason Conf, Can 1994;3:1433–42.
[137] Vimala S, Kumarasamy K. Studies on the strength of stabilized mud block masonry using different mortar proportions. Int J Emerg Technol Adv Eng 2014;4(4):720–4.
[138] Vindhyashree, Rahamath A, Kumar WP, Kumar MT. Numerical simulation of masonry prism test using ANSYS and ABAQUS. Int J Eng Res Technol 2015;4(7):1019–27.
[139] Vyas U, Reddy V. Prediction of solid block masonry prism compressive strength using FE model. Mater Struct 2010;43:719–35. https://doi.org/10.1617/s11527-009-9524-9.
[140] Wang N, Zhao X, Zhao P, Zhang Y, Zou Z, Ou J. Automatic damage detection of historic masonry buildings based on mobile deep learning. Autom Constr 2019;103:53–66. https://doi.org/10.1016/j.autcon.2019.03.003.
[141] Yang K-H, Lee Y, Hwang Y-H. A stress-strain model for brick prism under uniaxial compression. Adv Civ Eng 2019;2019:1–10. https://doi.org/10.1155/2019/7682575.
[142] Zahra T, Thamboo J, Asad M. Compressive strength and deformation characteristics of concrete block masonry made with different mortars, blocks and mortar beddings types. J Build Eng 2021;38:102213.
[143] Zavalis R, Jonaitis B, Lourenço P. Experimental investigation of the bed joint influence on mechanical properties of hollow calcium silicate block masonry. Mater Struct 2018;51:85.
[144] Zhou Q, Wang F, Zhu F. Estimation of compressive strength of hollow concrete masonry prisms using artificial neural networks and adaptive neuro-fuzzy inference systems. Constr Build Mater 2016;125:417–26. https://doi.org/10.1016/j.conbuildmat.2016.08.064.